Journal of Medicinal Chemistry

Article

Late Stage Lead Diversification (LSLD) Coupled with Quantitative NMR Spectroscopy to Identify New SAR Vectors at Nanomole Scale Synthesis: Application to Loratadine a Human Histamine H Receptor Inverse Agonist

Manjinder S. Lall, Asser Bassyouni, James Bradow, Maria Brown, Mark W Bundesmann, Jinshan Chen, Gregory Ciszewski, Anne Hagen, Dennis Hyek, Stephen Jenkinson, Bo Liu, R. Scott Obach, Senliang Pan, Usa Reilly, Neal W. Sach, Daniel Smaltz, Douglas K. Spracklin, Jeremy Starr, Melissa Wagenaar, and Gregory S Walker

J. Med. Chem., **Just Accepted Manuscript** • DOI: 10.1021/acs.jmedchem.0c00483 • Publication Date (Web): 28 May 2020

Late Stage Lead Diversification (LSLD) Coupled with Quantitative NMR Spectroscopy to Identify New SAR Vectors at Nanomole Scale Synthesis: Application to Loratadine a Human Histamine H_1 Receptor Inverse Agonist

Manjinder S. Lall,*[1] Asser Bassyouni,[2] James Bradow,[1] Maria Brown,[1] Mark Bundesmann,[1] Jinshan Chen,[1] Greg Ciszewski,[1] Anne E. Hagen,[1] Dennis Hyek,[3] Stephen Jenkinson,[2] Bo Liu,[3] R. Scott Obach,[1] Senliang Pan,[1] Usa Reilly,[1] Neal Sach,[2] Daniel J. Smaltz,[4] Douglas K. Spracklin,[1] Jeremy Starr,[1] Melissa Wagenaar,[1] Gregory S. Walker[1]

Corresponding Author:

*E-Mail**:** manjinder.lall@pfizer.com

[1]Pfizer Worldwide Research and Development, Eastern Point Road, Groton, Connecticut 06340, United States

[2]Pfizer Worldwide Research and Development, Science Center Drive, San Diego, California 92121, United States

[3]Spectrix Analytical Services, LLC, 410 Sackett Point Road, Bldg 20, North Haven, Connecticut 06473, United States

[4]Pfizer Worldwide Research and Development, 1 Portland Street, Cambridge, Massachusetts 02139, United States

ABSTRACT: An experimental approach is described for late stage lead diversification (LSLD) of frontrunner drug candidates using nanomole scale amounts of lead compounds for SAR development. The process utilizes C–H bond activation methods to explore chemical space by transforming candidates into newly functionalized leads. A key to success is the utilization of micro-cryoprobe NMR spectroscopy which permits the use of low amounts of lead compounds (1-5 μmoles). The approach delivers multiple analogs from a single lead at nanomole scale amounts as DMSO-d6 stock solutions with known structure and concentration for *in vitro* pharmacology and ADME testing. To demonstrate the feasibility of this approach, we have used the antihistamine agent loratadine (**1**). Twenty-six analogs of loratadine were isolated and fully characterized by NMR. Informative SAR analogs were identified which display potent affinity for the human histamine H_1 receptor and improved metabolic stability.

KEYWORDS: late stage lead diversification (LSLD) • late stage functionalization (LSF) • diversity focused synthesis (DFS) • positive/negative structure-activity relationship (+/-SAR) • miniaturization, nanoscale • drug discovery • C–H bond activation • liver microsomes • cytochrome P450 • microorganisms • metalloporphyrins • electrochemistry • Minisci reaction • Baran Diversinates • photoredox catalysis • micro-cryoprobe NMR • tandem mass spectrometry (MS/MS) • pharmacology testing • loratadine

INTRODUCTION

Late stage lead diversification (LSLD) is emerging as a powerful synthetic strategy for drug discovery.[1] This approach leverages unactivated C–H bonds as sites to incorporate functional groups or small substituents late in the synthetic route of a lead molecule by applying biochemical and chemical functionalization methods (Figure 1A).[2] From a medicinal chemist's perspective, lead diversification is a highly attractive approach because it does not require chemical pre-functionalization of starting materials or *de novo* synthesis for each new analog targeted. Furthermore, because pharmacological activity is already present in the lead molecule LSLD has the ability to rapidly and cost-effectively incorporate drug-like properties and attributes into promising candidates. Allowing the medicinal chemist to expand structure-activity relationship (SAR) knowledge, optimize ligand-target potency and selectivity, alter absorption-distribution-metabolism-excretion (ADME) properties, improve physicochemical properties like solubility, identify metabolically labile sites to aid drug design, access new and synthetically challenging unexplored chemical space and uncover novel intellectual property (IP) space. Therefore, this approach can significantly accelerate the drug discovery process with minimal synthetic investment, time and cost.

Drug discovery and development is challenging because most drugs are designed through iterative rounds of chemical synthesis and pharmacological testing to incorporate drug-like attributes into lead molecules.[3] The LSLD approach is appealing given that drug-like chemical space has been estimated at 10^{60} for molecules obeying Lipinski's rule-of-five for oral bioavailability and at 10^{20}-10^{24} for molecules up to 30 atoms.[4] To manage these formidable numbers, LSLD lends itself to methodology that favors diversity focused synthesis (DFS) where the aim is to explore a dense area of chemical space adjacent to regions known to have useful

properties, such as biological activity (Figure 1B).[5] Hence, library size is not as important as libraries with focused diversity with favorable physicochemical properties (e.g. LipE)[6] for a particular biological target.[7]

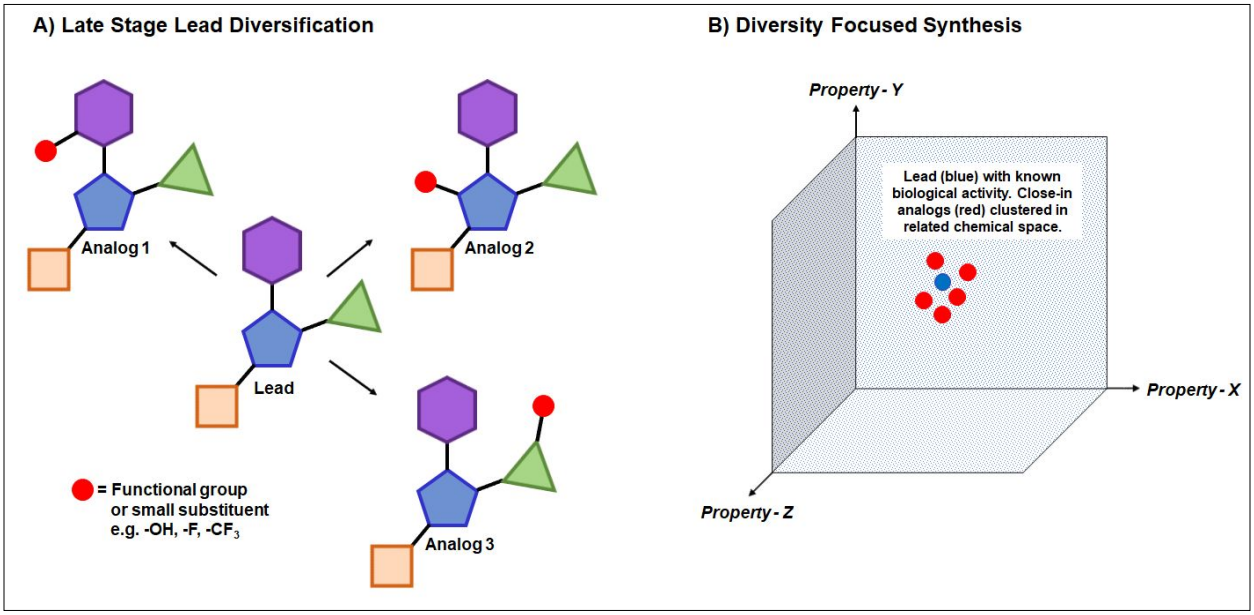

Figure 1. A) Late stage lead diversification (LSLD) to generate lead diversity in an efficient manner for a specific biological target. B) Diversity focused synthesis (DFS) explores related areas of chemical space in proximity to regions known to have useful properties.

Much attention has recently been focused on late stage C–H bond activation and functionalization methods to diversify lead molecules in drug discovery.[8] Incorporating functional groups or small substituents efficiently with judicious range in size and polarity into drug-like molecules is highly relevant for SAR development, can accelerate analog preparation and could potentially reduce high attrition associated with pharmaceutical research.[9a] For example, high lipophilicity of drug candidates can lead to poor oral absorption, low compound solubility and high metabolic turnover.[9b] Late stage C–H bond modification of biologically active compounds is an effective approach to address these issues because direct replacement of C–H bonds with

functional groups or substituents can significantly improve target binding or favorably influence receptor selectivity. Previously, we have described biosynthetic methods to carry out lead diversification and drug metabolite synthesis coupled with quantitative micro-cryoprobe NMR spectroscopy[1b-d,10] which laid the foundation for the present work. Herein, we report the operationalization and expansion of an approach to facilitate late stage lead derivatization and metabolite synthesis for advanced lead molecules using small amounts (i.e. 1-2 mg) of compound to support drug discovery. The approach generates chemical diversity of lead molecules through an alternative approach to classical medicinal chemistry practices, for rapid SAR knowledge and chemical space exploration. In particular, the approach utilizes direct C–H bond functionalization methods in support of diversity focused synthesis to transform candidates into newly substituted leads or noteworthy metabolites, such as: mammalian liver microsomes and cytosols;[1b-d] microorganisms;[11] engineered and recombinant P450 enzymes;[10,12] biomimetic metalloporphyrins;[13] electrochemistry;[14] Minisci chemistry;[15] alkyl sulfinate radical precursor chemistry (Baran Diversinates);[16] and photoredox catalysis.[17] Therefore, the approach enables 1) synthetic modification of lead compounds to improve biological properties; and 2) synthesis of metabolites for *in vitro* profiling to inform intrinsic clearance (CL_{int}) parameters. Key to our method is the underpinning analytical infrastructure which uses low amounts of lead compounds to carry out screens for hit identification, scale-up of interesting products, purification using liquid chromatography with automated fraction collection for isolation, full structure characterization based on high resolution mass spectrometry plus tandem mass spectrometry (MS/MS) and NMR spectroscopy utilized for both structure elucidation and quantitation (Figure 2). With little investment up-front (1-2 mg of lead), the approach delivers multiple analogs from a single lead at nanomole scale amounts (~5-10 μg per product) as DMSO-d6 stock solutions with known structure

and concentration for immediate pharmacology and ADME testing. The approach can rapidly and cost-effectively address multiple medicinal chemistry problems on miniaturized scale, such as: provide valuable +/-SAR information, improve potency and selectivity, identify metabolically labile sites to aid drug design, alter physicochemical properties and access novel synthetically challenging chemical space. To demonstrate our approach, we have generated compound diversity and drug metabolites using the antihistamine agent loratadine (**1**) as a prototypical compound to traverse through our workflow with the aim to explore chemical space about the A-D ring systems and identify new SAR vectors.

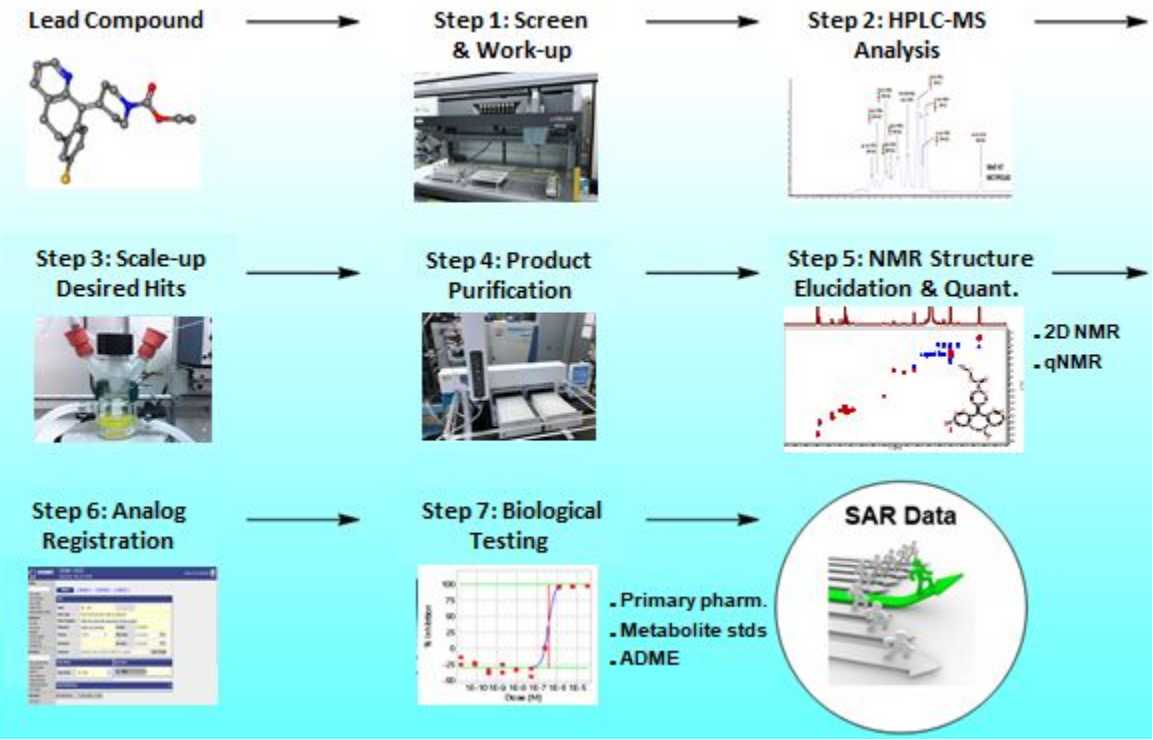

Figure 2. Workflow for late stage lead diversification.

RESULTS AND DISCUSSION

The clinical agent loratadine is a second generation antihistamine drug used to treat allergic rhinitis, also known as hay fever.[18] Well-known for more than 20 years, loratadine has been subject to extensive SAR.[19a-d] Loratadine is a tricyclic non-sedating inverse agonist of the human histamine H_1 receptor (dissociation constant, K_d = 0.19 μM) and is preferred over first generation antihistamines because of lack of sedation and CNS adverse effects.[19e-g] Loratadine was used as an example compound to test our approach and highlight the ability to generate diverse compounds because the molecule contains drug-like structural features common to typical lead molecules explored during drug discovery, such as sites containing: alkyl, O/N-alkyl, aryl, heteroaryl, carbonyl (carbamate), haloarene and unsaturation functionality (Figure 3). To explore loratadine SAR, we envisioned using various C–H bond activation methods to synthetically access and functionalize the A-D ring systems in **1**. The total synthesis of loratadine is complex and involves 7 steps with an overall yield of 37%, after considerable process development.[19a,b] Preparing SAR analogs of **1** with systematic and probing modification at all ring systems (A-D) in single transformative steps is challenging but conceivable using our approach.

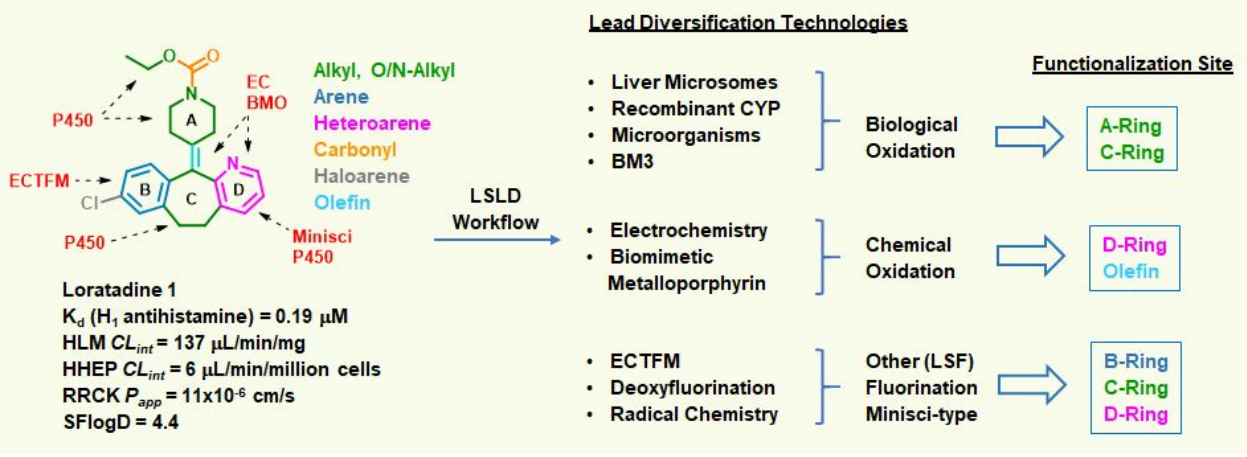

Figure 3. Functional group distribution of antihistamine drug loratadine (**1**) and lead diversification technologies employed for LSLD to access A-D ring system SAR.

Liver Microsomes and Recombinant CYP Enzymes: To diversify the alkyl sites in loratadine (A- and C-rings), compound **1** was screened against a panel of mammalian liver microsomes (9 systems) and human recombinant cytochrome P450 enzymes (9 CYP isoforms), configured in 96-well microtiter plate format for automated screening convenience as described in Table S1 in the Supporting Information section. Despite the large number of C–H bonds in loratadine, CYPs possess the exceptional capability to react at inert C(sp^3)–H bonds within carbon backbones preferentially over other more chemically reactive sites. Hence, cytochrome P450 enzymes are versatile chemo- and regioselective biocatalysts and are known to catalyze a wide range of reactions including but not exclusive to hydroxylation, O- and N-dealkylation, heteroatom oxidation, dehydrogenation and epoxidation.[20] Some of these transformations have the unique ability to introduce polarity (e.g. hydroxylation) at synthetically challenging sites and significantly lower lipophilicity; a single hydroxyl group adds 20 $Å^2$ of polar surface area (PSA) which can often lead to increased metabolic stability.[21] Furthermore, the hydroxyl group can behave as a hydrogen bond acceptor (HBA) or hydrogen bond donor (HBD) providing binding energy to biological targets resulting in increased ligand affinity. With these multifaceted capabilities, this functional group offers medicinal chemists a structural change that can modify a lead molecules behavior at the target site and in the body.[21b] As a result, the hydroxyl group is present in many biologically important molecules including ~20% of drugs[22a,b] and ~65% of natural products.[22c]

Accordingly, chromatographic profiles from liver microsomes and recombinant CYP screens (Table S2 in the Supporting Information) were examined by UV and tandem mass spectrometry (MS/MS) and the results evaluated for acceptable product yield (>10% conversion) and product diversity. It is important to mention that percent conversion to end-products as well as diversity of products are critical factors when considering which system should be selected for

scale-up. Also, reaction profiles which provide products in the molecular weight range of the starting material are favored over those which generate lower molecular weight product fragments via heteroatom dealkylation reactions. For loratadine, thirteen products were detected by HPLC-MS (Figure 4) where M+/-number refers to the average mass change difference between parent and analog (i.e. delta mass). The HPLC-MS results from the liver microsome and recombinant CYP screen show wells 9 and 18 generating good diversity, affording up to ten unique products with reasonable conversion. Products generated from wells 9 and 18 correspond to incubations with human liver microsomes and recombinant CYP3A4 (respectively) which is in good agreement with previous reports that show CYP3A4 and CYP2D6 as the predominant enzymes involved in loratadine *in vitro* metabolism.[23]

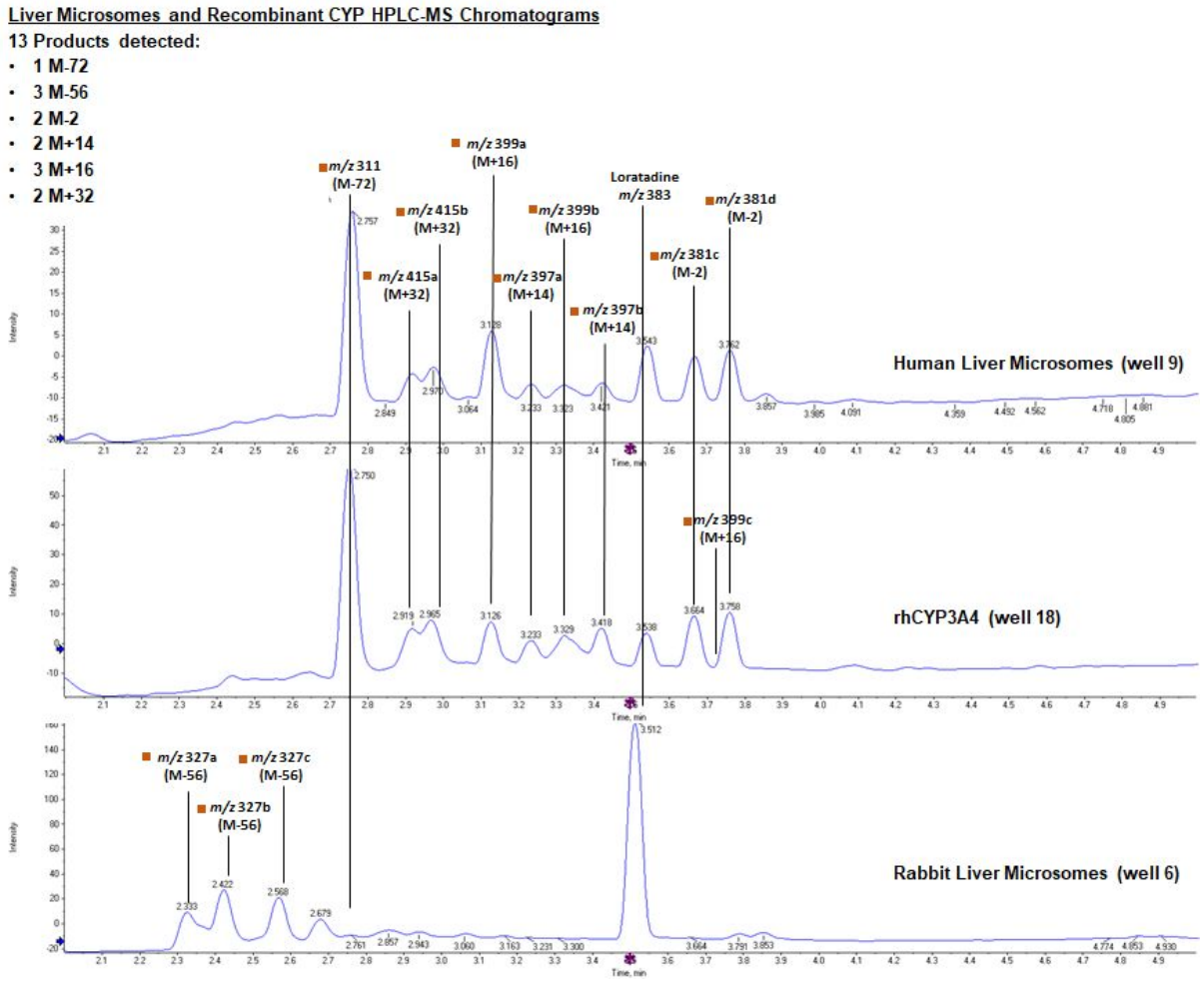

Figure 4. Liver microsomes and recombinant CYP HPLC-MS chromatograms for human liver microsomes (well 9), rhCYP3A4 (well 18) and rabbit liver microsomes (well 6). M+/-number refers to the average mass change difference between parent and analog (i.e. delta mass).

Screening lead molecules using liver microsomes in concert with recombinant CYPs, as in Table S1, also provides a prospective opportunity to forecast CYP liability and determine which isoforms are most active *in vitro*; offering an early glimpse into metabolite profiling and identification (Met ID).[24] Furthermore, we have established protein-ligand docking protocols based on known CYP isoform X-ray structures to guide potential binding modes of leads with CYP active sites using binding energy and shape complementarity scores.[25] Caution should be

used when utilizing protein-ligand docking to explain metabolism because of the highly dynamic nature of the P450 enzyme binding pocket. Thus, these initiatives are predictive but can potentially address drug design approaches to enhance metabolic stability given that a high rate of metabolism (i.e. high intrinsic clearance, CL_{int}) is a function of enzyme maximum velocity (*Vmax*) and the Michaelis constant (*Km*) (Figure 5).[26a] In view of this, metabolic clearance by P450s can be impacted through lead diversification strategies that block sites of metabolism, alter ligand electronics or introduce polarity into lead molecules.[26b]

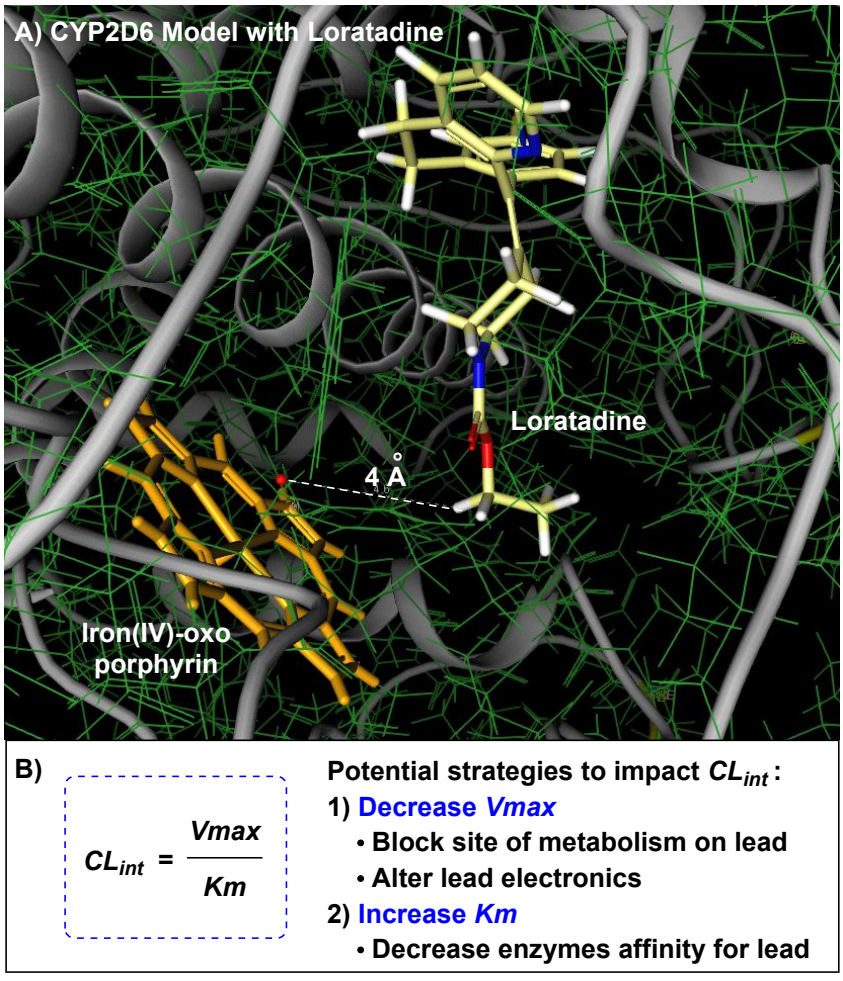

Figure 5. A) Modeled pose of loratadine with human CYP2D6. The oxygen atom of the CYP2D6 iron(IV)-oxo porphyrin radical cation is 4 Å from one of the methylene hydrogen atoms of the

ethyl carbamate moiety in loratadine. B) Potential strategies to alter a lead molecule's intrinsic clearance (CL_{int}) value.

Microorganisms: Microbes have long been an important source of bioactive natural products for drug discovery, providing a wealth of novel scaffolds as well as marketed drugs.[11,27] Most recently, microbial incubations with lead molecules have been investigated to chemically diversify drug candidates to expand SAR knowledge or incorporate chemical handles for further structural modification.[28] Other virtues of microbial biotransformations include their ability to mimic mammalian metabolism or produce microbe specific metabolites. They often produce multiple products, can generate compounds difficult to produce through synthetic chemistry, are scalable processes (mg to kg quantities), produce oxidative (phase I) and conjugative (phase II) metabolites and are cost-effective.[29] Thus, loratadine was screened for modification on ring systems A and C using a panel of 79 microorganisms which included organisms from bacteria, fungi and actinomycetes (Table S3 in the Supporting Information).

Loratadine was incubated with microbial panel (Table S3) to afford twenty-three products observed by HPLC-MS (Table S4 in the Supporting Information). As expected when using live whole cells, the microbial screen gave many products from phase I and II metabolism of loratadine. In addition, we observed non-drug related secondary metabolite products (e.g. M+63, M+65, M+84 and 2M+96) which can be differentiated from **1** by MS/MS fragmentation patterns. Of the twenty-three compounds detected, eighteen products appeared to be drug related by HPLC-MS (Figure 6).[30a] In considering the chromatographic profiles generated for loratadine using microbial whole cells, it was observed that bacterial organisms (e.g. well 19, *Nocardia* ATCC 21271a: 10 products detected) were more efficient at generating diversity as compared to fungal strains (e.g. well 65, *Mucor rouxii* UC7470: 6 products detected).[30b]

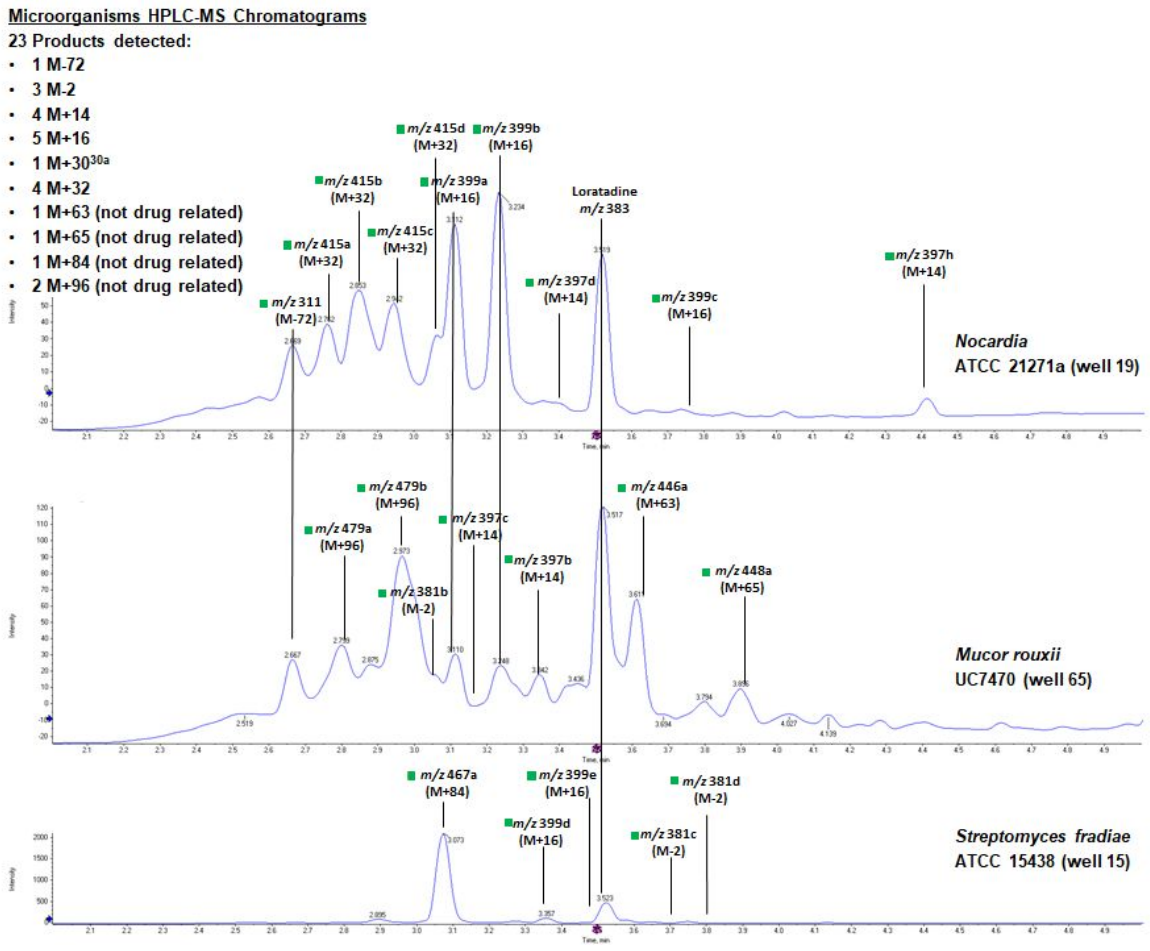

Figure 6. Microorganisms HPLC-MS chromatograms for *Nocardia* ATCC 21271a (well 19), *Mucor rouxii* UC7470 (well 65) and *Streptomyces fradiae* (well 15).[30a] M+/-number refers to the average mass change difference between parent and analog (i.e. delta mass).

Engineered Cytochrome P450 Enzymes: Mammalian cytochrome P450 (CYP) enzymes are a superfamily of membrane-bound heme containing monooxygenases that can insert atmospheric oxygen into unactivated C(sp^3)–H bonds across an enormous variety of substrates under mild conditions with a high degree of chemo- and regioselectivity.[31] Despite these noteworthy qualities, mammalian CYP applications are limited because of low turnover rate, enzyme instability and they acquire electrons through a complex process involving cytochrome P450 reductase and NADPH. For these reasons, there is considerable interest in utilizing directed evolution[32] to

engineer bacterial cytochrome P450 enzymes for the synthesis of novel drugs and drug metabolites.[33]

Bacterial cytochrome P450 enzymes can be evolved to afford new biocatalysts with enhanced synthetic applications to generate unique products not observed by mammalian CYPs and provide valuable +/-SAR for drug discovery. Cytochrome P450 from *Bacillus megaterium* CYP102A1 (P450 BM3) has characteristics that enable protein engineering for use in synthesis because it is expressed in *E. coli* at high levels, it is a soluble enzyme and its electron transfer and reductase domains are fused in one continuous polypeptide chain to efficiently facilitate oxidative transformations.[12,34] In this respect, tailoring the functionality of P450 BM3 has enabled its utility as an effective biocatalytic tool in pharmaceutical research with wide-ranging synthetic applicability from early drug discovery on small scale[35] to late development on kilogram scale.[36] With these salient features in mind, we utilized a cytochrome P450 BM3 panel comprised of 45 Codexis[37] variants selected for their ability to cover the reactivity scope of human CYPs by producing mammalian drug metabolites and also to show broad specificity on drug-like substrates to provide new diverse chemical leads (Table S5 in the Supporting Information).

To this end, loratadine was screened against our P450 BM3 panel and evaluated for enzyme functionalization activity and variety in product distribution about the A-, C- and D-ring systems. As expected, the reactivity scope of the 45-membered P450 BM3 panel was broad and produced a variety of products when applied against loratadine (Table S6 in Supporting Information), providing a product profile that complemented the mammalian liver microsome and recombinant CYP screen by generating different products. Seventeen different products were identified in the HPLC-MS chromatograms of select P450 BM3 reactions with **1** as substrate (Figure 7). The chromatographic traces from wells 40 (MCYP0012) and 47 (MCYP0160) show good diversity

profiles, generating up to sixteen products. A few of the P450 BM3 derived products matched retention times and MS/MS fragmentation patterns to those which arose from mammalian CYPs, which speaks to the panel's capability to prepare authentic drug metabolites. In addition, several BM3 variants gave products not observed when screening liver microsomes and recombinant CYPs underscoring their utility for lead diversification. Several BM3 enzymes displayed good degrees of regioselective-hydroxylation as exhibited by yielding five chromatographically different M+16 products (*vide infra*). These enzymes which give rise to single hydroxylation products are vital to SAR development because they effectively probe the lead molecule's ability to tolerate polar functionality at various sites, aiding drug design strategies for improved properties (e.g. target potency, solubility, oral bioavailability, etc.).[38] Furthermore, there was low occurrence of bis-hydroxylation which reflects the enzyme's exquisite selectivity for **1** over its more polar hydroxylated products limiting the synthesis of unwanted poly-hydroxylated compounds.

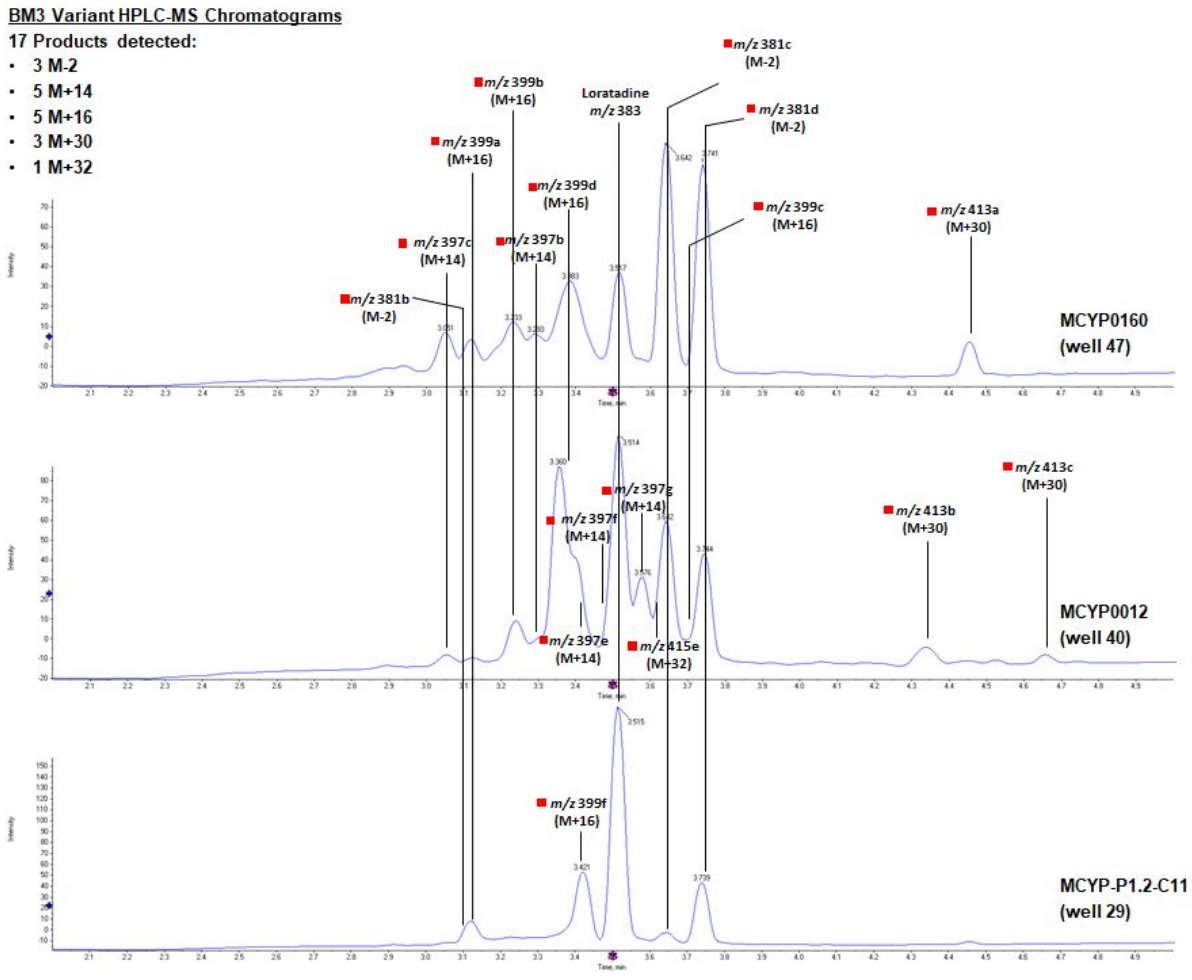

Figure 7. BM3 variant HPLC-MS chromatograms for MCYP0160 (well 47), MCYP0012 (well 40) and MCYP-P1.2-C11 (well 29). M+/-number refers to the average mass change difference between parent and analog (i.e. delta mass).

Electrochemistry: Electrochemical transformations are a simple and green method for enabling C–H bond functionalization of lead molecules, where addition or removal of electrons across an electrical potential can bring about lead modification or metabolite synthesis.[14] The advantage of electrochemistry is the ability to precisely control both the potential and rate of the redox process in a manner not possible with conventional chemical oxidants or reductants. For example, electrochemical functionalization has been used to prepare derivatives of the antibiotic tylosin

where modification of the parent compound gives rise to novel desmycosin analogs.[39] Electrochemical oxidation is also a useful tool to understand and study metabolic pathways, as demonstrated for the antimalarial drug amodiaquine.[40] To accommodate our needs we used a NuVant EZStat Pro potentiostat to acquire cyclic voltammetry (CV) readings to determine redox properties. Of particular interest is the initial anode oxidation potential which provides voltage parameters for the subsequent electro-oxidation reaction. As a result, a preparative undivided electrochemical cell was used to screen **1** (Figure S1A in the Supporting Information). Loratadine was subjected to electrolysis with constant potential (5 V) across the two electrodes to modify the olefinic region which flanks rings A and C in the molecule.

After electrochemical initiation, the reaction progress was monitored by HPLC-MS to follow formation of products. The reaction profile showed the formation of ten distinct products (Table S7 in the Supporting Information). The observed electrochemical products appeared unique by HPLC-MS (Figure 8) compared to products derived from biological oxidation (i.e. liver microsomes, recombinant CYP, microorganisms and BM3). This illustrates differences between the transformational methods and shows good complementarity between chemical and biological oxidative technologies to deliver a diverse set of products.

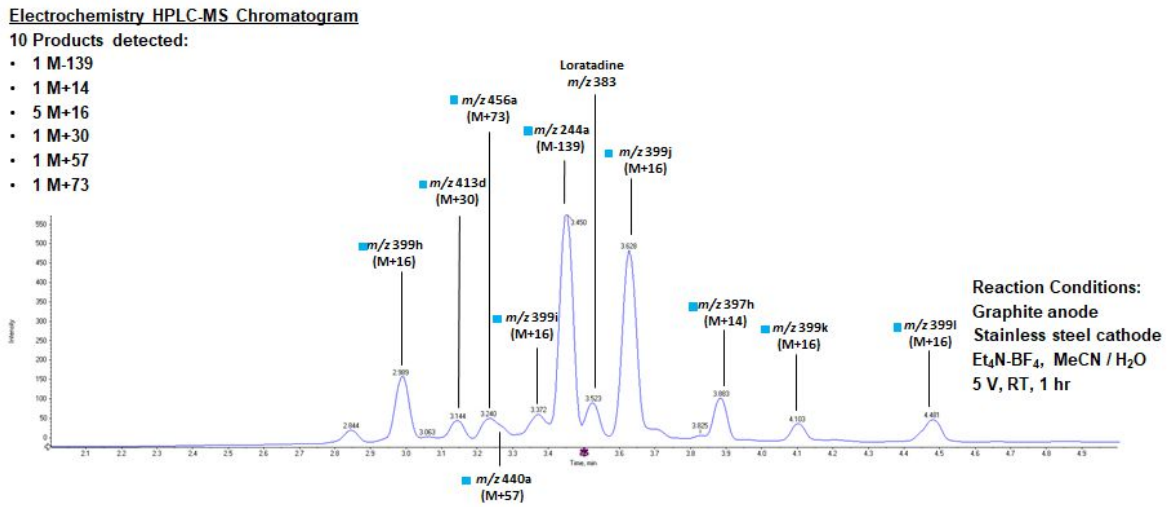

Figure 8. Electrochemistry HPLC-MS chromatogram. Electrolysis reaction conditions: graphite anode, stainless steel cathode, Et_4N-BF_4, 5 V, MeCN / H_2O, RT, 1 hr. M+/-number refers to the average mass change difference between parent and analog (i.e. delta mass).

Biomimetic Metalloporphyrin Oxidation: Synthetic metalloporphyrins capable of mimicking the selective C–H bond oxidation of heme containing monooxygenase cytochrome P450s have become of increasing significance to drug discovery in recent years.[41] These biomimetic metalloporphyrin oxidation (BMO) catalysts have been extensively investigated for lead diversification and metabolite synthesis.[42] Consequently, this method has been utilized for aliphatic hydroxylation,[43] O- and N-dealkylation, S- and N-oxidation and epoxidation, in addition to other transformations.[44] In view of this, loratadine was screened against a 120-membered BMO panel consisting of two solvent systems (MeOH / DCE or MeCN / DCE), six oxidants (PhIO, H_2O_2, Oxone, CHP / imidazole, *m*CPBA, or CHP / imidazole / HCO_2H) and nine commercially available metalloporphyrins[45] ((Fe(TNO_2PP), Mn(TFPP), Fe(TFPP), Cu(TFPP), Co(TFPP), Pd(TDCIPP), Mn(TDCIPP), Cu(TDCIPP) or Co(TDCIPP)) (Table S8 in the Supporting Information). The requisite screen was run under protic (MeOH / DCE, 1:1) and aprotic (MeCN / DCE, 1:1) solvent conditions, in an attempt to diversify the olefinic portion of loratadine and the

D-ring system. To ensure metalloporphyrin was actively participating in product formation a control screen was run with solvent and oxidant, but no metalloporphyrin.

Chromatographic profiles from the BMO screen were evaluated by HPLC-MS and showed the formation of six products (Table S9 in the Supporting Information). Once again the products derived from the BMO screen appeared distinct by retention time and MS/MS fragmentation pattern (Figure 9) from products derived from biological oxidation, indicating good complementarity between chemical and biological oxidation techniques to enable lead diversification.

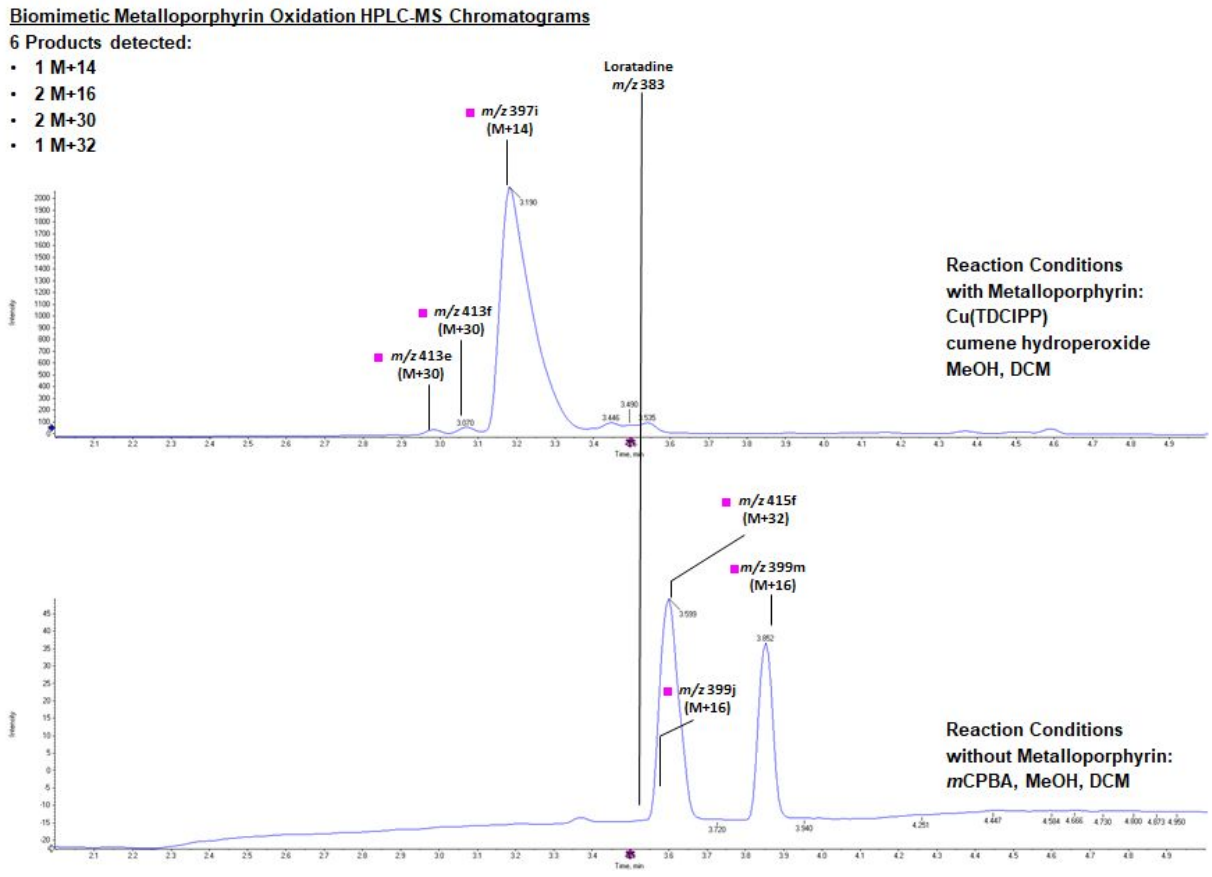

Figure 9. Biomimetic metalloporphyrin oxidation HPLC-MS chromatograms. Top chromatogram: reaction conditions with metalloporphyrin Cu(TDCIPP), cumene hydroperoxide,

MeOH, DCM. Bottom chromatogram: reaction conditions without metalloporphyrin, *m*CPBA, MeOH, DCM. M+/-number refers to the average mass change difference between parent and analog (i.e. delta mass).

Comparison of Lead Diversification Screens. With the HPLC-MS results in hand from all screens, we were able to compare and contrast chromatographic profiles from the different lead diversification and metabolite synthesis technology screens. Early on, it became apparent that chromatographic profiles derived from biological oxidative methods (i.e. liver microsomes, recombinant CYP, microorganisms and BM3) gave similar product profiles by LC retention time and MS/MS fragmentation, albeit with different product conversions (Figure 4, 6 and 7) which is important for scale-up considerations. These results were in stark contrast to chromatographic profiles obtained from EC and BMO screens (Figure 8 and 9), which gave relatively distinct products. Only one product, as determined by LCMS analysis, was generated in both the EC and BMO screens (e.g. *m/z* 399j, M+16) (Figure 9). Furthermore, the comparable *m/z* 399j product was generated in the control BMO well without metalloporphyrin suggesting loratadine is modified by oxidant *m*CPBA and not metalloporphyrin.

We also compared product similarity and difference relative to each biological technology by using a diversity map where screening panels from all biological systems (e.g. liver microsomes, recombinant CYP, microorganisms and BM3) are plotted as a function of product detected by HPLC-MS (Figure 10, see Excel S1_Diversity Map in the Supporting Information section to view entire plot). Viewing the data in this manner allowed for systematic identification of transformational systems which gave comparable products and, more importantly, to pinpoint systems which generate good product diversity.

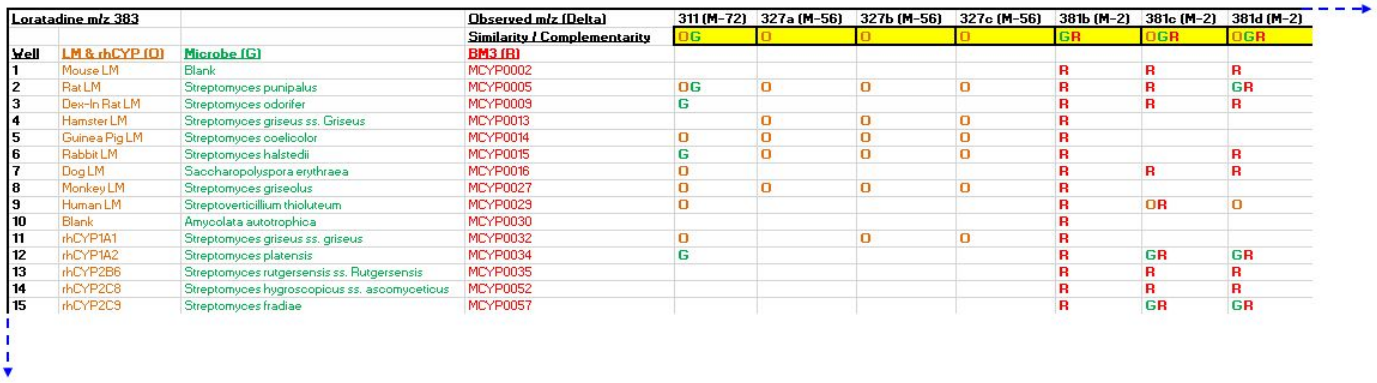

Loratadine m/z 383			Observed m/z (Delta)	311 (M-72)	327a (M-56)	327b (M-56)	327c (M-56)	381b (M-2)	381c (M-2)	381d (M-2)
			Similarity / Complementarity	OG	O	O	O	GR	OGR	OGR
Well	LM & rhCYP (O)	Microbe (G)	BM3 (R)							
1	Mouse LM	Blank	MCYP0002					R	R	R
2	Rat LM	Streptomyces punipalus	MCYP0005	OG	O	O	O	R	R	GR
3	Dex-In Rat LM	Streptomyces odorifer	MCYP0009	G				R	R	R
4	Hamster LM	Streptomyces griseus ss. Griseus	MCYP0013		O	O	O	R		
5	Guinea Pig LM	Streptomyces coelicolor	MCYP0014	O	O	O	O	R		
6	Rabbit LM	Streptomyces halstedii	MCYP0015	G	O	O	O	R		R
7	Dog LM	Saccharopolyspora erythraea	MCYP0016	O				R	R	R
8	Monkey LM	Streptomyces griseolus	MCYP0027	O	O	O	O	R		
9	Human LM	Streptoverticillium thioluteum	MCYP0029	O				R	OR	O
10	Blank	Amycolata autotrophica	MCYP0030					R		
11	rhCYP1A1	Streptomyces griseus ss. griseus	MCYP0032	O		O	O	R		
12	rhCYP1A2	Streptomyces platensis	MCYP0034	G				R	GR	GR
13	rhCYP2B6	Streptomyces rutgersensis ss. Rutgersensis	MCYP0035					R	R	R
14	rhCYP2C8	Streptomyces hygroscopicus ss. ascomyceticus	MCYP0052					R	R	R
15	rhCYP2C9	Streptomyces fradiae	MCYP0057					R	GR	GR

Figure 10. Diversity map of product similarity and difference relative to biological technology screened by HPLC-MS, refer to (Excel S1_Diversity Map) in the Supporting Information to view entire map. X-axis displays product distribution determined by HPLC-MS, shown in yellow (top); Y-axis displays well distribution from each biological screening panel: liver microsomes and recombinant CYP (shown in brown), microorganisms (shown in green) and BM3 variants (shown in red).

For example, extensive biotransformation of loratadine is observed from the diversity map using human liver microsomes (well 9) which generates nine products by HPLC-MS (*m/z* 311 (M-72), 381c (M-2), 381d (M-2), 397a (M+14), 397b (M+14), 399a (M+16), 399b (M+16), 415a (M+32) and 415b (M+32)). In a complimentary manner, the map also reveals four of these products (*m/z* 381c (M-2), 381d (M-2), 399a (M+16) and 399b (M+16)) are also made by microorganism *Streptomyces violascens* ATCC 31560 (well 27) and BM3 variant MCYP0012 (well 40). Figure 10 also uncovers that products (*m/z* 327a (M-56), 327b (M-56) and 327c (M-56)) are generated by rabbit liver microsomes (well 6), product (*m/z* 413c (M+32)) is made by microbe *Streptomyces setae* ATCC 33774[46] (well 28), and products (*m/z* 397f (M+14), 397g (M+14), 413b (M+30) and 415e (M+32)) are generated by BM3 variant MCYP0012 (well 40).

We further summarized the results from the diversity map to illustrate the distribution of similar products generated from the biological screens. For instance, liver microsome and recombinant CYP products observed by HPLC-MS were compared to the those generated by other biological technology screens e.g. microorganisms and BM3 (Figure 11). The results illustrated in Figure 11 show loratadine products generated from liver microsomes and recombinant CYPs have 69% product similarity to products generated from the microbial panel, 46% product similarity to products generated from the BM3 panel and 46% similarity to all panels. For a more comprehensive breakdown of product similarity relative to the other technologies screened by HPLC-MS refer to Table S10 in the Supporting Information.

Technology Screen	LM & rhCYP Product Similarity Relative to Other Technologies by HPLC-MS	
LM & rhCYP[1] (13 Products)[2]	Microbe[3] / LM & rhCYP[1] (9/13, 69%)[5]	BM3[4] / LM & rhCYP[1] (6/13, 46%)[5]

[1]LM & rhCYP screen = 9 liver microsomes, 9 recombinant CYPs.
[2]Number of LM & rhCYP products detected by HPLC-MS.
[3]Microbe screen = 79 microorganisms.
[4]BM3 screen = 45 *Bacillus megaterium* variants.
[5]Ratio of similar products detected relative to biological screen.

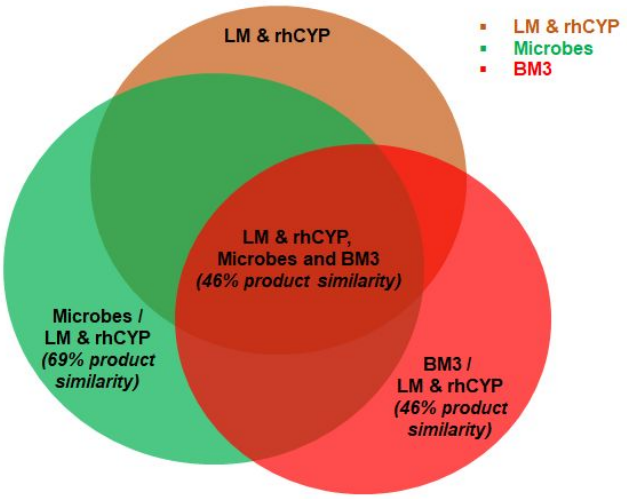

Figure 11. Ratio of liver microsome and recombinant CYP products observed by HPLC-MS relative to similar products detected from other technology screens (e.g. microbes and BM3). Venn diagram representation (bottom).

Lead Diversification Product Scale-Ups. With the diversity map in place, we shifted our attention to using the plot to select wells for product scale-up with a focus on lead diversification of loratadine with the specific aim to explore SAR chemical space by isolating products with modifications on rings A-D. For instance, Figure 10 shows rabbit liver microsomes (well 6) capable of converting loratadine to three unique products (*m/z* 327a-c, M-56) which are not observed in any of the other technology screens. Therefore, male rabbit liver microsomes (New Zealand, Xenotech) were selected for product scale-up which involved scaling the original liver microsomes screen conditions by a factor of 80-fold at a protein concentration of 2 mg/mL and substrate (**1**) concentration of 20.0 μM. Consequently, loratadine was incubated at 37 ^{o}C utilizing a reactor open to the atmosphere. After 1 hour, the reaction mixture was quenched with acetonitrile, centrifuged and adsorbed onto a C18 HPLC column. The column was transferred to a UHPLC instrument in line with a mass spectrometer and the products eluted using a 0.1% formic acid in water / acetonitrile gradient. Fractions containing peaks of interest were analyzed by UHPLC-UV-HRMS plus tandem mass spectrometry (MS/MS). The isolated samples were characterized by multidimensional NMR spectroscopy (COSY, HSQC and HMBC) using a 1.7 mm MicroCryoProbe[47] and quantified by external calibration against a benzoic acid standard solution applying ERETIC2.[48] As a result, descarboethoxy alcohols **2** (7.98 μg, 24.0 nmol) and **3** (2.22 μg, 6.8 nmol) were generated where modification occurred on the A- and C-rings of loratadine (Table 1). It is worth mentioning the isolable nanomole scale quantities of **2** and **3** are typical and manageable amounts for our workflow which permits rapid synthesis and pharmacological testing on miniaturized scale using nominal amounts of staring material (e.g. 306 μg of **1**), reagents and solvent. Descarboethoxy alcohols **2** and **3** are known human metabolites of loratadine.[49] Compound **2** was found to be a potent inverse agonist of human histamine H_1 receptor

with a dissociation constant of 48 nM, effectively 4-fold more active then loratadine (K_d = 190 nM). Remarkably, the regioisomeric alcohol **3** (K_d = 28 nM) is 7-fold more potent then loratadine. In addition, compounds **2** and **3** show slightly improved human hepatocyte stability compared to loratadine (1.75 and 3.14 μL/min/million cells vs. 6.1 μL/min/million cells), possibly the result of decreased lipophilicity reflected by the lower SFlogD values.[50] Interestingly, we also observed good passive permeability of **2** and **3** (RRCK P_{app} = 79.9 and 78.4 x 10^{-6} cm/sec, respectively). It is important to recognize that we did not determine absolute stereochemical configuration of the hydroxyl group for **2** and **3** and for all subsequent loratadine analogs generated herein. Nevertheless, from an SAR chemical space viewpoint analogs **2** and **3** indicate a basic amine is tolerated on the A-ring of loratadine and polarity is accepted at the C(sp^3)–H sites of the C-ring.

Table 1. SAR of Loratadine Analogs Generated from Rabbit Liver Microsomes.

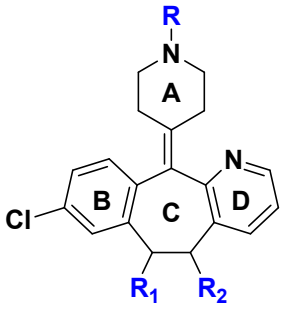

Compound	R	R_1	R_2	K_d^{α}	HLM$^{\beta}$ / HHEP$^{\gamma}$	RRCK$^{\delta}$	SFlogD$^{\varepsilon}$
Loratadine (**1**)	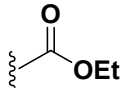	H	H	190	137 / 6.1	11.2	4.6
2	H	OH	H	48	ND / <1.75	79.9	0.94

3	H	H	OH	28	ND / 3.14	78.4	1.1

[α]Human histamine H_1 receptor dissociation constant (nM). Geometric mean of three replicates.

[β]Human liver microsome intrinsic clearance CL_{int} (μL/min/mg).

[γ]Human hepatocyte intrinsic clearance CL_{int} (μL/min/million cells).

[δ]Apparent passive permeability in the Ralph Russ Canine Kidney cell line P_{app} (10^{-6} cm/sec).

[ε]Shake-flask logD.

ND = Not determined.

We next focused on isolating a diverse pool of A- and C-ring analogs generated from our microbial screen. The diversity map shows microorganisms *Cunninghamella elegans* ATCC 8688a (well 73), *Streptomyces violascens* ATCC 31560 (well 27) and *Streptomyces setae* ATCC 33774 (well 28) are proficient at producing products (*m/z* 311, M-72), (*m/z* 399a, M+16), (*m/z* 399b, M+16) and (*m/z* 415c, M+32). Therefore, we initiated product scale-ups with these three microorganisms, which involved inoculating cultures from the previously mentioned microbes. After two days of culture growth, the incubate was charged with **1** (5 mg, 13 μmol) and the incubation was continued. The reaction mixtures were quenched and subjected to purification and characterization. Consequently, microorganism *Cunninghamella elegans* ATCC 8688a gave **4** (574 μg, 1847 nmol) as the A-ring altered descarboethoxy analog (Table 2). Compound **4** is recognized as a known metabolite of loratadine[23,51] and an approved second generation tricyclic antihistamine drug identified as desloratadine,[52] which displays potent affinity for the H_1 receptor (K_d = 24 nM). The C-ring positional hydroxyl-isomers **5** (27 μg, 67 nmol) and **6** (11 μg, 27 nmol) were generated from *Streptomyces violascens* ATCC 31560 and are not reported in the literature which speaks to the ability of our approach to deliver novel chemical matter for drug discovery. Hydroxyl analog **5** (K_d = 454 nM) was less active then its regioisomer **6** (K_d = 257 nM) which

maintained H_1 potency. Compound **6** also shows 2-fold improved permeability RRCK P_{app} = 26 x 10^{-6} cm/sec compared to **1** (RRCK P_{app} = 11 x 10^{-6} cm/sec). Based on the SAR results of **5** and **6**, it appears C-ring modification is better tolerated without the A-ring carboethoxy group as previously shown with congeners **2** and **3** which illustrates the receptor's high degree of selectivity. Lastly, microorganism *Streptomyces setae* ATCC 33774 afforded A-ring modified dicarbinolamide **7** (43 μg, 103 nmol), which is an unreported analog of loratadine. The stability of **7** was examined at several pH values (e.g. pH 1.2, 7.4 and 10.0) and the compound was found to be unchanged over 24 hours by HPLC-MS (Figure S2 in the Supporting Information). The dicarbinolamide functional group can be chemically prepared via a Hofmann rearrangement.[53] To our delight, compound **7** was found to have favorable potency (K_d = 51 nM) and better metabolic stability in human liver microsomes (HLM CL_{int} = 21 μL/min/mg) in comparison to loratadine (HLM CL_{int} = 137 μL/min/mg). In addition, the human hepatocyte values for **7** (HHEP CL_{int} = 13 μL/min/million cells) and **1** (6 μL/min/million cells) are similar and reflect good cellular metabolic stability. Importantly, loratadine analogs **5**, **6** and **7** are new compounds and underscore the capability of our approach to access novel chemical space coupled with new SAR vectors for medicinal chemistry teams to explore from a single transformational step.

Table 2. SAR of Loratadine Analogs Generated from Microorganisms.

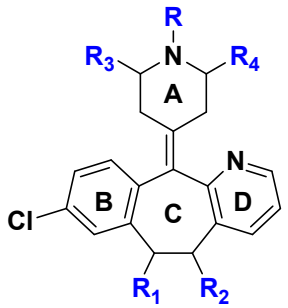

Compound	R	R_1	R_2	R_3	R_4	K_d[α]	HLM[β] / HHEP[γ]	RRCK[δ]	SFlogD[ε]
4[ζ]	H	H	H	H	H	24	4.8 / 6.5	2.8	1.3
5[η]	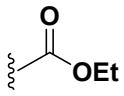	H	OH	H	H	454	132 / 61.5	23.7	3.3
6[η]	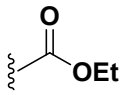	OH	H	H	H	257	157 / 40	26.2	3.2
7[θ]	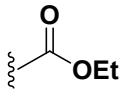	H	H	OH	OH	51	21 / 14	19.8	2.3

[α]Human histamine H_1 receptor dissociation constant (nM). Geometric mean of three replicates.

[β]Human liver microsome intrinsic clearance CL_{int} (μL/min/mg).

[γ]Human hepatocyte intrinsic clearance CL_{int} (μL/min/million cells).

[δ]Apparent passive permeability in the Ralph Russ Canine Kidney cell line P_{app} (10^{-6} cm/sec).

[ε]Shake-flask logD.

[ζ]From *Cunninghamella elegans* ATCC 8688a.

[η]From *Streptomyces violascens* ATCC 31560.

[θ]From *Streptomyces setae* ATCC 33774.

We applied our protein-ligand docking protocols of known CYP isoforms (e.g. CYP1A2, 2C8, 2C9, 2C19, 2D6 and 3A4) to analog **7** with the aim to understand the nature of the improved HLM metabolic stability compared to loratadine. Evaluating the CYP2D6 model with analog **7** as shown in Figure 12, we observe the oxygen atom of the iron(IV)-oxo porphyrin radical cation to be 13 Å from the methylene hydrogen atom of the ethyl carbamate group in **7** placing this moiety

of the molecule far from the CYP active site which could explain the lower intrinsic clearance value.[54] From a loratadine drug design perspective, the protein-ligand model suggests that introducing polar functionality adjacent to the carbamate nitrogen atom on the A-ring can improve metabolic stability. The diversity map shows compound **7** was not detected by HPLC-MS in the BM3 or liver microsomes and recombinant CYP screens.

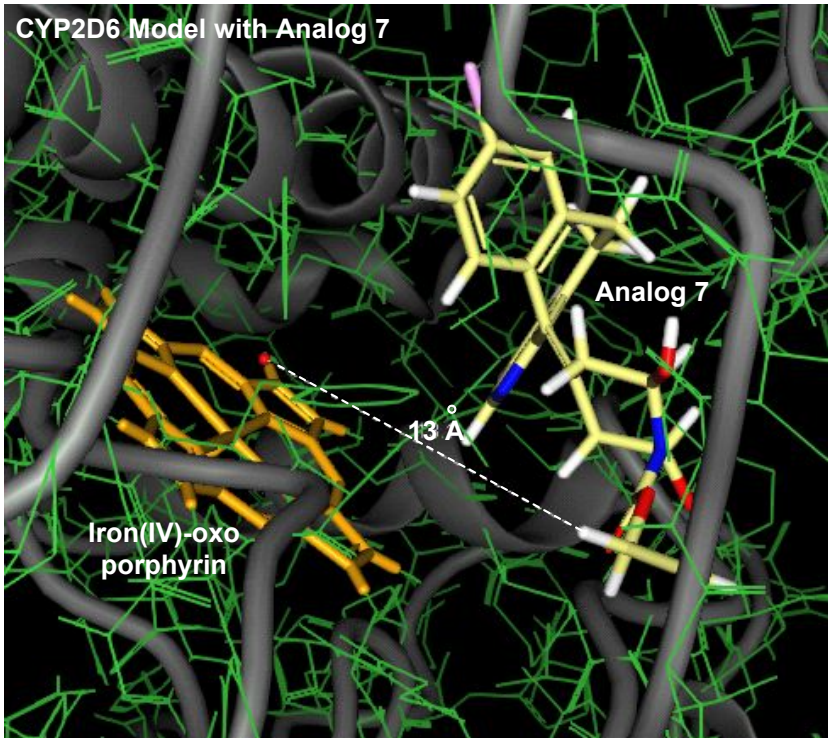

Figure 12. Modeled pose of analog **7** with CYP2D6. The oxygen atom of the CYP2D6 iron(IV)-oxo porphyrin radical cation is 13 Å from one of the methylene hydrogen atoms of the ethyl carbamate moiety in **7**.

With access to analog **5**, we attempted to explore the C-ring vector and restore activity by synthesizing the fluorinated congener via a deoxyfluorination reaction using the reagent *N,N*-diethylaminosulfur trifluoride (DAST).[55] We have found deoxyfluorination of hydroxylated compounds an effective strategy for drug design to optimize ligand-target potency, selectivity and

improve metabolic stability. Due to fluorine's small size (van der Waals radius 1.47 Å) and large electronegativity (3.98 Pauling scale), introduction of a fluorine atom can dramatically impact a compounds conformation, pKa and cell permeability.[56] For these reasons, fluorine is present in a large and growing number of approved drugs (~25%).[57] Moreover, fluorination at the site of cytochrome P450 modification can lower the rate of metabolic turnover or alter the site of metabolism, hence fluorine substitution is a viable approach to mitigate drug metabolism.[10a] Therefore, alcohol **5** was treated with DAST (Scheme 1). After work-up, the crude material was purified to afford C-ring fluorinated analog **8** (25 μg, 62 nmol). We were pleased to see the H_1 activity restored in compound **8** (K_d = 227 nM) with equivalent HLM CL_{int} (120 μL/min/mg), RRCK P_{app} (13x10^{-6} cm/s) and SFlogD (4.5) to loratadine. However, the human *in vitro* hepatic metabolic stability of **8** (HHEP CL_{int} = 32 μL/min/million cells) was increased by 5-fold compared to **1** (HHEP CL_{int} = 6 μL/min/million cells), possibly due to a change in site of metabolism or the result of increased lipophilicity. Also, we cannot overlook the importance of how metabolism rate can be influenced by stereochemistry, bearing in mind that the individual enantiomers of **8** could have different metabolic rates which we have not investigated.

Scheme 1. Synthesis of Compound 8.

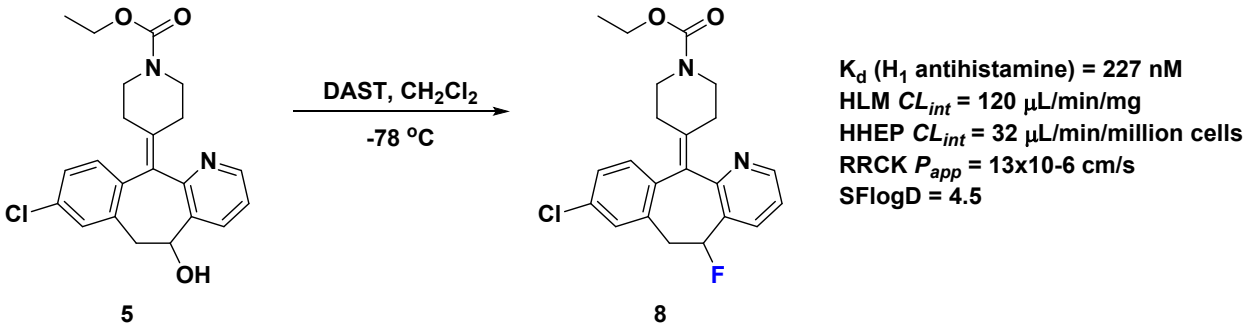

The 45-membered P450 BM3 screen identified several enzymes that are active against **1** and capable of functionalizing rings A and C (Figure 10). In particular, the diversity map uncovered enzymes MCY0012 (well 40) and MCYP0160 (well 47) as giving a substantial number of products (16 detected) with diverse profiles compared to the other lead diversification screens, as determined by HPLC product retention time and MS/MS fragmentation pattern. As a result, the BM3 screening conditions for wells 40 (MCY0012) and 47 (MCY0160) were scaled by a factor of 200-fold to give a final protein concentration of 1-2 mg/mL and substrate (**1**) concentration of 250.0 μM. After reaction with BM3 enzymes, the crude material was submitted for purification to afford analogs **9**-**17** (Table 3) in isolated yields ranging from 10 to 200 μg. As predicted from the diversity map enzymes MCYP0012 and MCYP0160 provided a generous degree of A-, C- and D-ring structural diversity. The products isolated included those with alkyl hydroxylation (**9** and **17**), heteroarene hydroxylation (**11**), unsaturation (**14**-**16**), as well as products with hydroxylation plus unsaturation (**10**, **12** and **13**). It is worth mentioning that access to analogs such as **9**-**17** using conventional synthetic methods would be challenging. Furthermore, upon structural elucidation we determined that a handful of these compounds were novel and not reported in the literature (**10**, **12**, **13**-**15** and **17**), in alignment with the goal to prepare analogs which evaluate unexplored chemical space and provide positive and negative SAR. The majority of BM3 derived analogs show poor binding affinity for the H_1 receptor apart from alcohol **9** (K_d = 423 nM) and olefin **15** (K_d = 454 nM).

Table 3. SAR of Loratadine Analogs Generated from BM3 Variants.

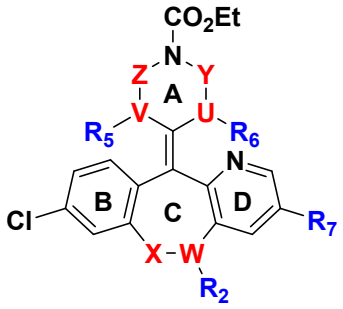

Cpd	R_2	R_5	R_6	R_7	Z-V	Y-U	X-W	K_d[α]	HLM[β] / HHEP[γ]	RRCK[δ]	SFlogD[ε]
9[φ,γ]	H	OH	H	H	CH_2-CH	CH_2-CH	CH_2-CH	423	51 / 19	22	3.1
10[ζ,η]	OH	H	H	H	CH=C	CH_2-CH	CH_2-CH	>1000	ND / 82	78	3.4
11[ζ]	H	H	H	OH	CH_2-CH	CH_2-CH	CH_2-CH	>1000	132 / 96	11	3.1
12[ζ]	H	H	H	OH	CH_2-CH	CH=C	CH_2-CH	>1000	61 / 62	ND	3.9
13[ζ]	H	H	H	OH	CH=C	CH_2-CH	CH_2-CH	>1000	66 / 67	ND	3.1
14[ζ]	H	H	H	H	CH=C	CH_2-CH	CH_2-CH	>1000	68 / ND	40	4.3
15[ζ,η]	H	H	H	H	CH_2-CH	CH=C	CH_2-CH	454	ND / ND	53	3.6
16[η]	H	H	H	H	CH_2-CH	CH_2-CH	CH=C	>1000	ND / 9	98	2.6
17[ζ]	H	OH	OH	H	CH_2-CH	CH_2-CH	CH_2-CH	>1000	35 / 18	23	2.8

[α]Human histamine H_1 receptor dissociation constant (nM). Geometric mean of three replicates.

[β]Human liver microsome intrinsic clearance CL_{int} (μL/min/mg).

[γ]Human hepatocyte intrinsic clearance CL_{int} (μL/min/million cells).

[δ]Apparent passive permeability in the Ralph Russ Canine Kidney cell line P_{app} (10^{-6} cm/sec).

[ε]Shake-flask logD.

[φζ]From MCY0012.

[γη]From MCYP0160.

ND = Not determined.

From a structural point of view, we were intrigued with heteroaromatic modified analogs **11**-**13** and wondered if alternate substituents on the D-ring of loratadine might be tolerated. Alkyl sulfinate salts, also known as Baran Diversinates, have recently emerged as radical precursors for direct incorporation of alkyl substituents onto heteroarene systems to facilitate late stage functionalization (LSF) of lead compounds.[16,58] Accordingly, the synthesis of difluoromethyl analogs of loratadine were pursued by treating **1** with difluoromethanesulfinate zinc salt in the presence of *tert*-butyl hydroperoxide (TBHP) oxidant under acidic conditions (TFA). Employing these prescribed conditions, we obtained novel D-ring substituted regioisomers **18** (1.0 mg, 2.3 μmol) and **19** (1.2 mg, 2.7 μmol). As shown in Table 4, CHF_2 substituted analog **18** displays no activity against the histamine H_1 receptor (K_d >1000). However, the positional isomer **19** exhibits good affinity for H_1 (K_d = 271 nM) and points out the importance of this D-ring SAR vector. However, the metabolic stability of **19** appears compromised (HLM CL_{int} = 283 μL/min/mg, HHEP CL_{int} = 40 μL/min/million cells). The CHF_2 group can behave as a lipophilic hydrogen bond donor. From a drug design perspective, we thought lowering the logD of compounds like **19** (SFlogD = 3.2) might provide leads with improved intrinsic clearance. In addition, the CHF_2 substituent has been used as a bioisostere for thiols, hydroxamic acids, amides and hydroxyl groups.[59] For that reason, we targeted the addition of a hydroxymethyl group to the D-ring of loratadine. Treating **1** with Rongalite (sodium hydroxymethanesulfinate) under standard reaction conditions, furnished the desired hydroxymethyl regioisomer **20** (142 μg, 344 nmol). As desired, analog **20** is less lipophilic (SFlogD = 2.6) then **19** (SFlogD = 3.2) and impressively maintains potent affinity for the H_1 receptor (K_d = 199 nM). Unfortunately, an improved metabolic profile

was not seen with hydroxymethyl **20** (HLM CL_{int} = 283 µL/min/mg, HHEP CL_{int} = 59 µL/min/million cells).

Table 4. SAR of Loratadine Analogs Generated from Alkyl Sulfinate Radical Precursor.

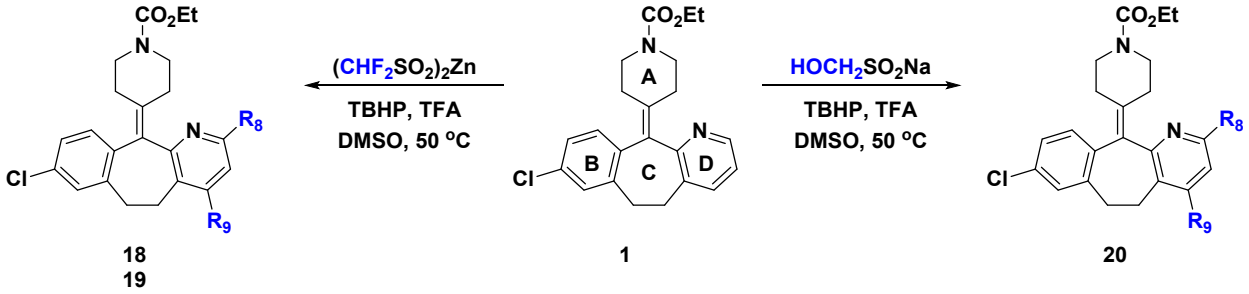

18
19

1

20

Compound	R_8	R_9	K_d^{α}	HLM$^{\beta}$ / HHEP$^{\gamma}$	RRCK$^{\delta}$	SFlogD$^{\varepsilon}$
18	CHF_2	H	>1000	108 / 48.7	7.7	4.6
19	H	CHF_2	271	283 / 39.8	4.5	3.2
20	H	CH_2OH	199	283 / 58.6	16.2	2.6

$^{\alpha}$Human histamine H_1 receptor dissociation constant (nM). Geometric mean of three replicates.

$^{\beta}$Human liver microsome intrinsic clearance CL_{int} (µL/min/mg).

$^{\gamma}$Human hepatocyte intrinsic clearance CL_{int} (µL/min/million cells).

$^{\delta}$Apparent passive permeability in the Ralph Russ Canine Kidney cell line P_{app} (10^{-6} cm/sec).

$^{\varepsilon}$Shake-flask logD.

With the successful demonstration of LSF applications to loratadine using Baran Diversinates, we next attempted to apply other known late stage functionalization chemistries to prepare additional analogs of **1**. For instance, photoredox catalysis has become a powerful method to efficiently install alkyl and halo groups into complex molecules.[60] Therefore, we subjected **1** to

photocatalytic decarboxylative alkylation conditions developed by Stephenson.[61] This proved unsuccessful in our hands and we only observed degradation of starting material. We also tried direct photocatalytic fluorination conditions pioneered by Britton using tungsten-based polyoxometalate catalyst TBADT, again we only detected starting material fragmentation and complex mixtures.[62] It is possible under these conditions the olefin moiety within loratadine is not compatible with productive photoredox alkylation or fluorination.

We subsequently shifted our attention to scaling products from the BMO and electrochemical screens. The biomimetic oxidative screen identified conditions containing the copper based Cu(TDCIPP) metalloporphyrin catalyst for scale-up consideration (Table S9 in the Supporting Information). As a result, the BMO reaction was scaled by treating substrate **1** with Cu(TDCIPP) at 10 mol% in the presence of cumene hydroperoxide oxidant. In addition, a control reaction was run on similar scale without metalloporphyrin catalyst (Cu(TDCIPP)) in the presence of oxidant. The crude materials from both reactions were subject to similar purification and characterization methods employed for the enzyme-based preparations. The control reaction without Cu(TDCIPP) metalloporphyrin catalyst gave olefin and D-ring altered known products **21** (0.4 mg, 0.96 μmol), **22** (1.8 mg, 4.34 μmol) and **23** (8.4 mg, 20.92 μmol) from *m*CPBA oxidation.[63a] Unfortunately, these three analogs showed poor H_1 receptor affinity (K_d >1000 nM) (Table 5). Apparently, modification of the olefin group or D-ring nitrogen atom of loratadine is not tolerated as revealed from the SAR of analogs **21**-**23**. As for the BMO product in the presence of metalloporphyrin catalyst Cu(TDCIPP), we isolated the *N*-methyl formate salt **24** (1.5 mg, 3.84 μmol) which also displayed poor binding affinity to the H_1 receptor.[63b]

Table 5. SAR of Loratadine Analogs Generated from Biomimetic Metalloporphyrin Oxidation (BMO).

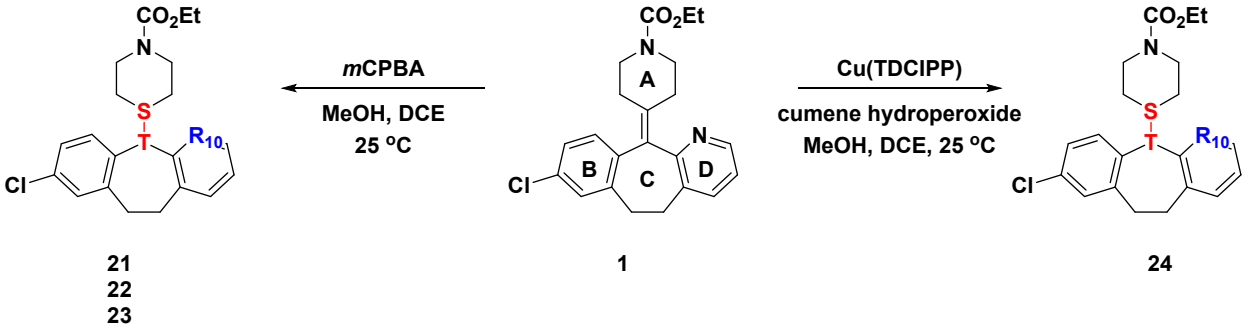

21
22
23

1

24

Compound	R_{10}	S | T	K_d^{α}	HLM$^{\beta}$ / HHEP$^{\gamma}$	RRCK$^{\delta}$	SFlogD$^{\varepsilon}$
21	N	O	>1000	89 / 26.2	17.9	2.9
22	O^- | N^+	O	>1000	<7 / 4.6	15.2	2.1
23	O^- | N^+	C = C	>1000	48 / 17.8	26.8	2.8
24$^{\zeta}$	CH_3 | N^+	C = C	>1000	23 / 6	0.2	0.3

$^{\alpha}$Human histamine H_1 receptor dissociation constant (nM). Geometric mean of three replicates.

$^{\beta}$Human liver microsome intrinsic clearance CL_{int} (μL/min/mg).

$^{\gamma}$Human hepatocyte intrinsic clearance CL_{int} (μL/min/million cells).

$^{\delta}$Apparent passive permeability in the Ralph Russ Canine Kidney cell line P_{app} (10^{-6} cm/sec).

$^{\varepsilon}$Shake-flask logD.

$^{\zeta}$Formate salt.

We next focused on scaling the products derived from electrochemistry. Using an undivided electrochemical cell, **1** was treated with Et_4NBF_4 solution in acetonitrile and water

(Figure S1A in the Supporting Information). The cell was charged for 1 hour at 5.0 V and monitored by HPLC-MS for the formation of products. Treatment of **1** under the aforementioned electrochemical conditions afforded epoxide **21** (1.1 mg, 2.75 μmol) and A-ring expanded ketone **25** (0.89 mg, 2.23 μmol) (Scheme 2). It is worth mentioning epoxide **21** is the same product isolated from the control BMO reaction (Table 5), which turns out to be the *m/z* 399j product also identified by HPLC-MS during the electrochemistry screen (Figure 8).[64]

Scheme 2. Synthesis of Loratadine Analogs Using Electrochemistry.

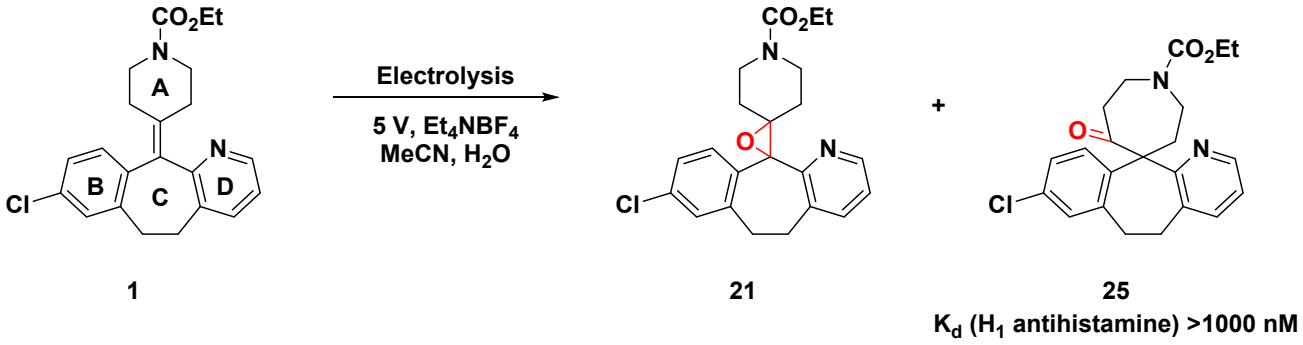

1 **21** **25**

K_d (H_1 antihistamine) >1000 nM

The ring expanded ketone **25** is novel and most likely the result of a House-Meinwald type rearrangement from epoxide **24**,[65] unfortunately analog **25** is not active against the H_1 receptor (Scheme 3). Nevertheless, serendipitous products such as **25** provide valuable SAR to medicinal chemistry teams and generate new chemical matter in a single step that would be challenging to synthesize using conversional methods.

Scheme 3. House-Meinwald Type Rearrangement.

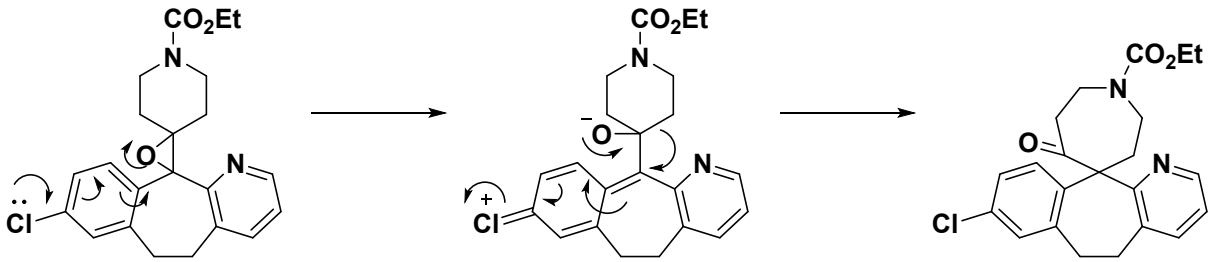

21 **25**

Having successfully modified many sites on the loratadine molecule we next moved to using electrochemistry as a facilitator to modify the B-ring of **1**. Electrochemical trifluoromethylation (ECTFM) initiated by sulfinate derived radicals has emerged as a method for synthesis of fluoroalkyl substituted arenes[66a,b] and heteroarenes.[66c] Accordingly, electrolysis of a solution of **1** (19 mg, 50 μmol) and sodium trifluoromethanesulfinate (NaTFMS) salt was carried out. Upon completion of the reaction, the crude material was purified to provide novel product **26** (83 μg, 184 nmol) as a 1:1 mixture of trifluoromethyl regioisomers substituted at the 7- and 9-position of the loratadine B-ring (Scheme 4). In addition, the electrochemical reaction afforded known deschloro-loratadine **27** (220 μg, 631 nmol). Trifluoromethyl analog **26** was tested as a 1:1 mixture of regioisomers and found to have moderate active against the H_1 receptor (K_d = 882 nM) and as expected the deschloro-loratadine analog **27** shows potent H_1 affinity (K_d = 208 nM).[67]

Scheme 4. Synthesis of Loratadine Analogs Using Electrochemical Trifluoromethylation.

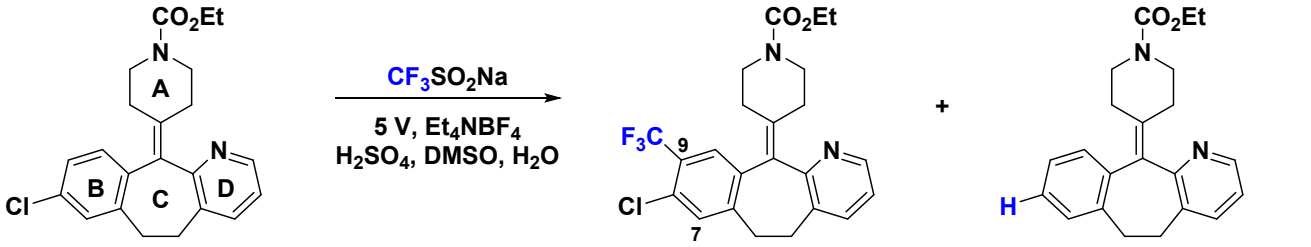

1 **26** **27**

1:1 mixture of 7-CF_3 and 9-CF_3 regioisomers

K_d (H_1 antihistamine) = 882 nM

K_d (H_1 antihistamine) = 206 nM

CONCLUSION

Late stage lead diversification coupled with quantitative NMR spectroscopy supports SAR exploration at the nanomole scale by introducing structural variation to molecules with established pharmacology, where the aim is to explore dense areas of chemical space adjacent to regions known to have useful properties. Conventional medicinal chemistry approaches to lead diversification requires multi-step synthesis and tens to hundreds of milligrams of starting materials to ensure adequate amounts of end-product are produced for pharmacological testing. We have enabled an approach which utilizes various C–H bond activation methods to diversify lead compounds in a single step at nanomole scale, minimizing synthetic investment, time and cost. By design this approach is promiscuous resulting in multiple analogs from a single lead, which are isolated and fully characterized at microgram levels. Applying this strategy to loratadine (**1**), over 40 products were detected by HPLC-MS analysis from lead diversification screens, which translated to 26 products isolated and characterized by NMR (product yield range: 0.01-1.0 mg). Consequently, 9 chemical transformations were observed with addition of polar and non-polar substituents across loratadine A-D rings encompassing: deacylation, hydroxylation, unsaturation,

epoxidation, N-oxidation / methylation, oxidative ring expansion, heteroaryl alkylation, fluoromethylation and dechlorination. Loratadine's chemical space was explored and positive SAR vectors were identified providing analogs equipotent to 8x more potent than parent through modification of the A-ring (analogs **4**, **7**), B-ring (analog **27**), C-ring (analogs **6**, **8**), D-ring (analogs **19**, **20**) and A/C-rings (analogs **2**, **3**). In addition, analogs **2**, **3**, **4** and **7** show comparable to 4x improved metabolic stability relative to parent. Furthermore, negative SAR was gained from several analogs which provides valuable pharmacophore information towards understanding the molecular recognition requirements needed between ligand and biological target. In summary, this work highlights the ability for late stage lead diversification to provide valuable +/-SAR information to medicinal chemistry teams and to alter crucial physicochemical properties of compounds for drug discovery. Applications using this approach to contemporary medicinal chemistry programs are underway and will be reported in due course.

EXPERIMENTAL SECTION

Materials. All commercially available materials and solvents were used as received unless otherwise stated. Loratadine (**1**), nicotinamide adenine dinucleotide phosphate (NADPH), *N,N*-diethylaminosulfur trifluoride (DAST), *meta*-chloroperoxybenzoic acid (*m*CPBA), cumene hydroperoxide (CHP, 80 wt. percent in H_2O), *tert*-butyl hydroperoxide (TBHP, 70 wt. percent in H_2O), difluoromethanesulfinate zinc salt, trifluoromethanesulfinate sodium salt, hydroxymethanesulfinate sodium salt (Rongalite), tetraethylammonium tetrafluoroborate (Et_4NBF_4) and 1,2-dichloroethane (DCE) were purchased from Sigma-Aldrich (St. Louis, MO) and used as is without further purification. Metalloporphyrins Fe(TNO_2PP), Mn(TFPP),

Fe(TFPP), Cu(TFPP), Co(TFPP), Pd(TDCIPP), Mn(TDCIPP), Cu(TDCIPP) and Co(TDCIPP) were obtained from Frontier Scientific (http://www.frontiersci.com/). Dimethyl sulfoxide-*d6* (DMSO-*d6*) was acquired from Cambridge Isotope Laboratories (Tewksbury, MA). Liver microsomes were purchased from the following vendors: female mouse, male rat, male cynomolgus monkey and non-transfected microsomes (Corning, Woburn, MA); dexamethasone-induced male rat, male hamster, male dog and pooled male & female human (prepared in-house at Pfizer, Groton, CT); and male guinea pig and male rabbit (Xenotech, Lenexa, KS). Note, human and monkey liver microsomes are considered biohazardous materials and appropriate precautions should be taken during handling and disposal. Recombinant human P450 enzymes heterologously expressed in microsomes from Sf9 cells were custom prepared by Panvera (Madison, WI). Cytochrome P450 BM3 variants and MCYP-RXN BUFFER were purchased from Codexis (Redwood City, CA). Sources of microorganisms: American Type Culture Collection (ATCC), Agricultural Research Service Culture Collection (NRRL - Northern Regional Research Laboratory), Institute for Fermentation (IFO), NITE Biological Resource Center (NBRC), and in-house cultures Ultra Cold (UC) and Calgary.

Equipment. Experimental procedures were generally carried out under inert atmosphere using nitrogen where oxygen or moisture sensitive reagents were used. Commercial solvents including anhydrous solvents and general reagents were used as is without additional purification and purchased from Sigma-Aldrich (St. Louis, MO). The following equipment was utilized in the preparations of final compounds unless otherwise stated: liquid chromatography mass spectrometry data are reported from a AB Sciex Triple TOF 5600+ mass spectrometer (Concord, Ontario, Canada) in line with a Agilent Technologies 1200 Series (Santa Clara, CA) comprised of

a vacuum degasser, binary pump SL, HiP-ALS high performance autosampler, TCC SL thermostatted column compartment and DAD (diode array detector) SL; AB Sciex Triple TOF 5600 mass spectrometer (Concord, Ontario, Canada) in line with a Waters Acquity UPLC system (Milford, MA) comprised of a PDA (photo diode array) detector, column manager FTN-1, sample organizer and binary solvent manager; Thermo Fisher Scientific Orbitrap Elite / Velos Pro mass spectrometer in line with a Accela PDA detector, 1250 pump and open autosampler (Waltham, MA); Thermo Fisher Scientific LTQ Velos mass spectrometer in line with a Waters Acquity UPLC system (Milford, MA) comprised of a PDA detector, column manager, sample manager, binary solvent manager and Leap Technologies PAL HCT-xt collector (Morrisville, NC); Thermo Fisher Scientific LTQ XL mass spectrometer in line with a Agilent 1100 Series HPLC system (Santa Clara, CA) comprised of a vacuum degasser, quaternary pump, ALS autosampler, Colcom column compartment, DAD (diode array detector) and 1260 Infinity FC-AS fraction collector. JASCO PU-1580 Intelligent HPLC pumps (Easton, MD). Eppendorf Thermomixer R (Hamburg, Germany). Thermo Fisher Scientific (Waltham, MA) Precision reciprocal shaking bath and Dubnoff Metabolic shaking incubator. Genevac EZ-2 Elite and HT-4X (Ipswich, Suffolk, England). Beckman Coulter Allegra 64R centrifuge (Brea, CA). Eppendorf 5424 and 5810R centrifuge (Hamburg, Germany). Thermo Fisher Scientific (Waltham, MA) HAAKE A10 circulating chiller and SC100 immersion circulator. IKA RCT Basic magnetic stir plate (Wilmington, NC). J-KEM Scientific DTC-4 multi-channel temperature controller with single-element thermocouple (St. Louise, MO). Wheaton Celstir jacketed flask 25-500 mL (Millville, NJ). Thermo Fisher Scientific MaxQ 2000 benchtop orbital shaker (Waltham, MA). New Brunswick Innova 4900 incline platform rotary shaker (Edison, NJ). Tecan Freedom Evo 150 automated liquid handler (Mannedorf, Switzerland).

General Screening Protocol Using Automated Liquid Handler. A Tecan Freedom EVO 150 automated liquid handler (Mannedorf, Switzerland) was used to streamline high-throughput screening, refer to the Tecan Protocol for Screening in the Supporting Information.

General High Performance Liquid Chromatography with Tandem Mass Spectrometry (HPLC-MS) Method for Screen Analysis. Screen samples were analyzed by HPLC-MS for acceptable conversion (>10%) and diversification of products using an AB Sciex Triple TOF 5600+ mass spectrometer in line with an Agilent Technologies 1200 Series HPLC instrument comprised of a vacuum degasser, binary pump SL, HiP-ALS high performance autosampler, TCC SL thermostatted column compatment and DAD (diode array detector) SL. Test samples were injected (5.0 μL) onto a C18 UHPLC column (HALO C18 UHPLC 3.0 x 50.0 mm, 2.7 μm) and a 0.1% formic acid in water (A) and 0.1% formic acid in acetonitrile (B) gradient was applied at a flow rate of 0.5 mL/min, maintained at 23 ^{o}C with a total run time of 6.5 minutes. The initial composition of 95%A/5%B was held for 0.3 minutes followed by a linear gradient to 5%A/95%B at 3.8 minutes, which was held to 5.0 minutes. The column was then re-equilibrated to the initial composition over 1.5 minute. Chromatograms of extracted λ = 286-291 nm were reconstructed from the diode array spectra for analysis. The mass spectrometer was operated in positive ion electrospray mode. Analyst TF™ software (AB Sciex, version 1.7.1) was used to control the LC/MS system. Source gases 1 & 2 were set to 50, DP = 70, capillary voltage = 5500 V and source temp = 500 °C. Full scan data were collected over 100-1000 amu at ~35,000 resolution and Information Dependent (IDA) Scan function criteria were used to collect the product ion spectra of the four most intense ions found in each survey scan. Data dependent scanning was used to

trigger MS2 analysis of molecular ions over a threshold intensity of 100 counts. Product ion spectra were acquired over a mass range of 100-1000 *m/z* with CE = 40 eV with a collision energy spread = 20 eV. Mass defect filters of potential loratadine analogs and cleavage products, based on elemental compositions, were prepared in Metabolite Pilot™ (AB Sciex, version 1.5) and transferred to the acquisition method. These MDF windows for loratadine analogs specific ions were placed in an inclusion list and applied during data acquisition to prioritize the collection of MS/MS spectra for those molecular ions meeting the MDF criteria, thereby focusing on drug related material to prioritize the acquisition of ions of interest. Peak View™ (AB Sciex, version 2.2) software was used to process data.

Ultra-Performance Liquid Chromatography Mass Spectrometry (UPLC-MS) Reaction Monitoring Conditions. Unless stated, reaction progress was monitored using a Waters SQ Detector 2 single-quadrupole atmospheric pressure ionization (API) mass spectrometer (ZSpray ESI/APCI/ESCi). In line with a Waters Acquity UPLC instrument comprised of a sample organizer, column manager, sample manager, binary solvent manager, PDA (photodiode array) detector λ = 200-400 nm TWC scan and ELS (evaporative light scattering) detector. Test samples were injected (2.0 μL) onto a Waters Acquity C18 UHPLC column (BEH 2.1 x 50.0 mm, 1.7 μm) and a 0.05% trifluoroacetic acid in water (A) and 0.0.5% trifluoroacetic acid in acetonitrile (B) gradient was applied at a flow rate of 0.8 mL/min, maintained at 23 ^{o}C with a total run time of 6.0 minutes. The initial composition of 5% B was increased by a linear gradient to 100% B over 4.0 minutes, which was held for 1.0 minute. The column was then re-equilibrated to the initial composition over 1.0 minute. Standalone Acquity Console and MassLynx V4.1 were used to control the UPLC-MS system.

General Chromatographic Purification Method 1. The 50 mL supernatant clear solution was adsorbed onto a C18 HPLC column (Zorbax Polaris, C18-A 250 x 4.6 mm, 5.0 μm) using a JASCO PU-1580 HPLC pump at a flow rate of 0.8 mL/min over ~60 minutes. The HPLC column was transferred to a Thermo LTQ Velos mass spectrometer in line with a Waters Acquity UHPLC instrument comprised of a quaternary pump, autosampler and photodiode array UV/vis detector. A gradient of 0.1% formic acid in water (A) and acetonitrile (B) was applied with a flow rate of 0.8 mL/min and run time of 110 minutes to separate products of interest. The initial conditions of 2% B, were increased to 10% B over 1.0 minute and held for 4.0 minutes, followed by an increase to 50% B over 85 minutes and then an increase to 95% B over 10 minutes, then return to the initial conditions over 10.0 minutes. After passing through the PDA detector, the eluent was split at a ratio of approximately 1:15 using a flow splitter (Advantage Flow Splitter model 62-4114, Analytical Sales & Services, Inc.) with the smaller portion going to the mass spectrometer and the larger portion to a fraction collector (Collect PAL, Leap Technologies); fractions were collected every 20 seconds. The collected fractions were analyzed by UHPLC-UV-HRMS using a Thermo Orbitrap Elite high-resolution ion trap mass spectrometer in line with a Thermo Accelar UHPLC and diode array UV/vis detector with a CTC Analytics Leap autoinjector (Thermo-Fisher). Samples were injected (2.0 μL) onto a C18 UHPLC column (Phenomenex Kinetex, C18 50 x 2.1 mm, 1.7 μm) and a 0.1% formic acid in water (A) and acetonitrile (B) gradient was applied at a flow rate of 0.4 mL/min, maintained at 45 ^{o}C. After UHPLC-UV-HRMS analysis, fractions of interest were pooled and the solvent was removed using an EZ-2 Elite Genevac (3 hour HPLC setting, 34 ^{o}C / 238 mbar to 41 ^{o}C / 7 mbar). Purity of all products was ≥95% unless otherwise noted.

General Chromatographic Purification Method 2. Crude samples were purified by preparative HPLC using an Agilent (Santa Clara, CA, USA) 1260 Infinity Prep LC-MS with the following components two Agilent G1361A preparative pumps, isocratic pump, refractive index detector, diode array detector VL, dual loop autosampler, single quadrupole mass spectrometer with Jetstream installed, universal interface box II and an active splitter. The instrument was controlled by ChemStation version C.01.05. A Phenomenex Gemini NX C18 column (21.1 x 250 mm, 5.0 μm) was used with flow rate of 25.0 mL/min at ambient temperature. A gradient consisting of 0.1% formic acid in water (A) and 0.1% formic acid in acetonitrile (B) was employed with the following gradient: initial conditions 5% B, hold for 1.50 minutes then increase solvent B to 90% over 24.5 minutes, hold for 3.0 min, then return to initial conditions over 1.0 minute. The UV data was collected at 210 or 215 nm and mass spectrometry data (ESi+) was collected using SIM on the target mass. Purity of all products was ≥95% unless otherwise noted.

General Chromatographic Purification Method 3. Crude samples were purified using preparative HPLC using a Waters (Milford, MA, USA) Auto-Purification FractionLynx LC-MS, coupled to a Waters 2545 binary gradient pump, 2767 fraction collector, 996 PDA and SQ2 single quadrupole mass spec detector. The instrument was controlled by MassLynx version 4.1. A Waters Sunfire C18 column (19 x 150 mm, 5.0 μm) was used with flow rate of 25.0 mL/min at ambient temperature. A gradient consisting of 0.05% trifluoroacetic acid in water (A) and 0.05% trifluoroacetic acid in acetonitrile (B) was employed with the following gradient: initial conditions 25% B to 37% B over 23.5 minutes, then 37% B to 100% B over 0.5 minutes, hold for

1.0 min, then return to initial conditions over 1.0 minute. The UV data was collected at 210 or 215 nm and mass spectrometry data (ESi+) was collected using the extracted ion on the target mass (ESi+; scan range 160-1000 daltons). Purity of all products was ≥95% unless otherwise noted.

Nuclear Magnetic Resonance Spectroscopy. All samples were placed in a vacuum chamber connected to a Vacuum Atmospheres Nexus II glove box and held at (-30 psi) for 1 hour or longer and then transferred to the glove box. The glove box was maintained under an atmosphere of argon with positive pressure. NMR samples were dissolved in "100%" DMSO-*d6* (45 μL) and charged into a 1.7 mm NMR tube. A Bruker Avance 600 MHz (Brucker BioSpin Corporation, Billerica, MA) NMR instrument equipped with a 1.7 mm TCI MicroCryoProbe was used, controlled by Topspin V3.2. One-dimensional spectra were recorded with an approximate sweep width of 8400 Hz and a total recycle time of approximately 7 seconds. To enhance adequate signal to noise, the resulting time-averaged free induction decays were transformed using an exponential broadening of 1.0 Hz. Two-dimensional spectra were recorded with the standard pulse sequence offered by Bruker. ^{1}H Proton and ^{13}C carbon spectra were referenced using residual DMSO-*d6* (^{1}H δ = 2.50 ppm relative to TMS, δ = 0.00, ^{13}C δ = 39.50 ppm relative to TMS, δ = 0.00). Chemical shift data is expressed in parts per million (ppm, δ) with multiplicities given as s (singlet), d (doublet), t (triplet), dt (doublet of triplets), q (quintet), m (multiple) and br (broad). Processing of post-acquisition data was completed with Topspin V3.2 or MestReNova V9.1 (Mestrelab Research, Santiago de Compostela, Spain). NMR samples were quantitated using the ^{1}H NMR spectrum of benzoic acid (5.0 mM) as external standard calibrant against the ERETIC2 function in Topspin V3.2.

Liver Microsomes and Recombinant CYP Enzyme Screen Procedure. Loratadine (20.0 μM, 10.0 nmol) was incubated with 9 mammalian liver microsomes (2.0 mg/mL) and 9 human recombinant P450 enzymes (2.0 mg/mL), as displayed in the plate format in Table S1 of the Supporting Information session. The total volume in each well was 0.5 mL which contained potassium phosphate buffer (0.1 M, pH 7.4), $MgCl_2$ (3.3 mM, 1.65 μmol) and acetonitrile (0.4% v/v). The reaction was initiated with the addition of NADPH (1.3 mM, 0.65 μmol) and agitated at 37 °C in a reciprocal shaking bath at 1" throw for 1 hour. The incubation was quenched with the addition of acetonitrile (1.5 mL), followed by centrifugation (1700 *g*, 5 min). The supernatant was removed and the solvent reduced using a Genevac centrifuge evaporator. The residue was reconstituted in 0.1 mL of 1% formic acid in H_2O / 20% acetonitrile, followed by centrifugation (1700 *g*, 5 min). The samples were analyzed using the General HPLC-MS Method for Screen Analysis.

Liver Microsomes Scale-Up Procedure for the Synthesis of Analogs 2 and 3. A 500 mL Erlenmeyer flask was charged with de-ionized water (27.04 mL) and treated with 1.0 M potassium phosphate buffer solution at pH 7.5 (4.0 mL), 0.165 M magnesium chloride solution (0.8 mL, 132 μmol) and a 0.005 M solution of compound **1** (0.16 mL, 0.8 μmol) in acetonitrile / water (1:1). The mixture was treated with liver microsomes (4.0 mL at 20 mg/mL) followed by the addition of a freshly prepared 0.013 M aqueous solution of NADPH (4.0 mL, 52 μmol). The uncapped Erlenmeyer flask was shaken using a Thermo Scientific Precision reciprocal shaker with a 1" throw at 37 °C for 1 hour. The reaction mixture was divided into equal portions (20 mL each) and poured into two 50 mL Falcon conical centrifuge tubes. The solutions were quenched by adding

acetonitrile (20 mL) to each Falcon tube. The Falcon tubes were vortexed and centrifuged at 1700 *g* for 5 minutes using a Centrifuge CT422 instrument. The supernatant was decanted and transferred in equal portions (20 mL each) to two 50 mL Falcon conical centrifuge tubes and the solvent was evaporated using a Genevac EZ-2 Elite (1 hour HPLC setting, 34 °C / 238 mbar to 41 °C / 7 mbar). The remaining aqueous solutions were combined (~20 mL) into a 50 mL Falcon conical centrifuge tube and treated with acetonitrile (0.5 mL), neat formic acid (0.5 mL) and charged with de-ionized water to a final volume of 50 mL. The solution was divided into equal portions (25 mL each) and poured into two high speed centrifuge tubes and centrifuged at 40,000 *g* for 30 minutes using a Beckman Coulter Allegra 64R (26200 speed, 24 °C) instrument. The supernatant was decanted into a 50 mL glass conical tube and the clear solution was subjected to General Chromatographic Purification Method 1. The dried samples were analyzed by NMR spectroscopy and quantified by external calibration against the ^{1}H NMR spectrum of a 5.0 mM benzoic acid standard solution in DMSO-d_6 using the ERETIC2 function within Topspin V3.2.

*8-Chloro-11-(piperidin-4-ylidene)-6,11-dihydro-5H-benzo[5,6]cyclohepta[1,2-b]pyridin-6-ol (**2**) and 8-chloro-11-(piperidin-4-ylidene)-6,11-dihydro-5H-benzo[5,6]cyclohepta[1,2-b]pyridin-5-ol (**3**).* Prepared from male rabbit liver microsomes (4.0 mL at 2 mg/mL, New Zealand, Xenotech) and a 5.0 mM solution of compound **1** (0.16 mL, 0.8 μmol) in acetonitrile / water (1:1). Yield of **2**: 7.98 μg, 24.0 nmol, 3%. Mixture of conformational isomers.[49] ^{1}H NMR (600 MHz, DMSO-d6) δ 8.41 – 8.38 (m, 1H), 7.86 – 7.79 (m, 1H), 7.33 – 7.17 (m, 3H), 7.13 – 7.11 (m, 1H), 5.20 (dd, *J* = 10.2, 4.6 Hz, 1H), 3.52 (dd, *J* = 16.6, 4.7 Hz, 1H), 3.15 – 3.08 (m, 2H), 2.85 – 2.80 (m, 3H), 2.51 – 2.23 (m, 3H), 2.22 – 2.19 (m, 1H); HRMS (TOF) Calcd for 327.1264, found 327.1267. Purity by HPLC-UV (288 nm) 97% using General Chromatographic Purification Method 1 (retention time = 2.643 min). Yield of **3**: 2.22 μg, 6.8 nmol, 0.9%. Mixture of

conformational isomers.[49] ^{1}H NMR (600 MHz, DMSO-d6) δ 8.44 – 8.35 (m, 1H), 7.90 – 7.77 (m, 1H), 7.36 – 7.18 (m, 3H), 7.17 – 7.09 (m, 1H), 5.20 (dd, *J* = 9.1, 4.5 Hz, 1H), 3.50 (dd, *J* = 17.3, 4.9 Hz, 1H), 3.19 – 3.05 (m, 2H), 2.94 – 2.78 (m, 3H), 2.54 – 2.34 (m, 3H), 2.28 – 2.15 (m, 1H).; HRMS (TOF) Calcd for 327.1264, found 327.1272. Purity by HPLC-UV (288 nm) 95% using General Chromatographic Purification Method 1 (retention time = 2.832 min).

Microorganism Screen Procedure. Microbial screening 96-well plates were prepared by adding previously grown or sporulated stocks of various actinomycetes, bacteria, or fungi, as shown in the plate format in Table S3 of the Supporting Information session to a sterile 96-well (2 mL each) plate. Plates were covered with a sterile cap mat and stored at -80°C until use. Sterile Iowa medium was prepared by combining dextrose (20.0 g, 0.1 mol), NutriSoy flour (5.0 g), NaCl (5.0 g, 0.085 mol), yeast extract (5.0 g), K_2HPO_4 (5.0 g, 0.029 mol), P2000 antifoam (1.0 ml) and deionized water (1.0 L, 55.3 mol), followed by adjusting the pH to 7.0 with 1.0 M HCl. The mixture was autoclaved to sterilize the media (25 min/L).

The 96 well microbial screening plate was thawed to room temperature (23 °C) and each well was treated with sterile Iowa medium (0.5 mL). The plate was covered with a sterile porous adhesive film (Thermo #241205: Nunc sealing tape; white rayon, breathable) and incubated using an Innova 4900 incline platform rotary shaker at 2" throw and 210 rpm, at a temperature of 30°C, for two days. A 13.0 mM solution of **1** (0.01 mL, 0.13 mmol) in DMSO was added to each well and the plate was covered with sterile adhesive porous film (Thermo #241205). The incubation was continued with rotary shaking (2" throw, 210 rpm) at 30°C for an additional 4 days. The reaction was terminated with the addition of acetonitrile (0.5 ml / well), followed by pipet aspiration and mixing using an Eppendorf Thermomixer R (650 rpm) at 30°C for ~20 minutes.

The plate was centrifuged with a Beckman Coulter Allegra instrument at 4000 *g* for 20 minutes and the supernatant was transferred to a new 96 well plate. The samples were analyzed using the General HPLC-MS Method for Screen Analysis.

Microorganism Scale-Up Procedure for the Synthesis of Analogs 4, 5, 6 and 7. Sterile Iowa medium (25 mL, as prepared above) was added to a sterile ventilated Nalgene flask (250 ml, #4116-0250) with baffle which was then inoculated with a stock suspension of microorganism culture (0.25 ml, contains 20% glycerol). The flask was capped and agitated on a 2" throw rotary shaker (Innova 4900, 210 rpm) at 30°C for two days. After 48 hours, the suspension was treated with a 13.0 mM solution of **1** (1.0 mL, 13.0 μmol) in DMSO. The flask was recapped and the incubation was continued as above for an additional 5 days. The incubation mixture was extracted with two volumes of ethyl acetate (2 x 50 mL) using a separatory funnel. The combined extracts were filtered through a bed of anhydrous magnesium sulfate and the filter cake was washed with ethyl acetate (20 mL). The solvent was removed using a rotary evaporator (42 °C) to a volume of less than 10 mL and the crude material was dried overnight *in vacuo*. The crude material was purified using General Chromatographic Purification Method 2. The dried samples were analyzed by NMR spectroscopy and quantified by external calibration against the ^{1}H NMR spectrum of a 5.0 mM benzoic acid standard solution in DMSO-d_6 using the ERETIC2 function within Topspin V3.2.

*8-Chloro-11-(piperidin-4-ylidene)-6,11-dihydro-5H-benzo[5,6]cyclohepta[1,2-b]pyridine (**4**).* Prepared from *Cunninghamella elegans* ATCC 8688a (0.25 ml stock suspension, contains 20% glycerol) and 13.0 mM solution of **1** (1.0 mL, 13.0 μmol) in DMSO. Yield of **4**: 574 μg, 1847 nmol, 14%. ^{1}H NMR (600 MHz, DMSO-d_6) δ 8.35 (d, J = 5.1 Hz, 1H), 7.58 (d, J = 7.8 Hz, 1H), 7.31 (s, 1H), 7.25 – 7.17 (m, 2H), 7.14 – 7.07 (m, 1H), 3.40 – 3.24 (m, 2H), 3.11 –

2.93 (m, 2H), 2.90 – 2.69 (m, 4H), 2.48 – 2.32 (m, 2H), 2.31 – 2.19 (m, 2H); HRMS (TOF) Calcd for 311.1315, found 311.1306. Purity by HPLC-UV (215 nm) 95% using General Chromatographic Purification Method 2 (retention time = 3.444 min).

*Ethyl 4-(8-chloro-5-hydroxy-5,6-dihydro-11H-benzo[5,6]cyclohepta[1,2-b]pyridin-11-ylidene)piperidine-1-carboxylate (**5**) and ethyl 4-(8-chloro-6-hydroxy-5,6-dihydro-11H-benzo[5,6]cyclohepta[1,2-b]pyridin-11-ylidene)piperidine-1-carboxylate (**6**).* Prepared from *Streptomyces violascens* ATCC 31560 (0.25 ml stock suspension, contains 20% glycerol) and 13.0 mM solution of **1** (1.0 mL, 13.0 μmol) in DMSO. Yield of **5**: 27 μg, 68 nmol, 0.5%. ^{1}H NMR (600 MHz, DMSO-d_6) δ 8.42 – 8.36 (m, 1H), 7.88 – 7.76 (m, 1H), 7.32 – 7.19 (m, 3H), 7.14 – 7.07 (m, 1H), 6.11 – 5.55 (m, br, 1H), 5.19 – 5.17 (m, 1H), 4.08 – 4.00 (m, 2H), 3.70 – 3.55 (m, 2H), 3.50 – 3.45 (m, 1H), 3.27 – 3.11 (m, 2H), 3.07 – 2.74 (m, 1H), 2.43 – 2.01 (m, 4H), 1.21 – 1.14 (m, 3H); HRMS (TOF) Calcd for 399.1475, found 399.1474. Purity by HPLC-UV (215 nm) 99% using General Chromatographic Purification Method 2 (retention time = 3.910 min). Yield of **6**: 11 μg, 28 nmol, 0.2%. ^{1}H NMR (600 MHz, DMSO-d_6) δ 8.38 – 8.30 (m, 1H), 7.77 – 7.43 (m, 2H), 7.27 (d, J = 8.0 Hz, 1H), 7.23 – 7.17 (m, 1H), 7.13 – 7.06 (m, 1H), 5.29 – 4.56 (m, 1H), 4.04 (q, J = 7.1 Hz, 2H), 3.76 – 3.56 (m, 2H), 3.50 – 3.33 (m, 1H), 3.27 – 3.12 (m, 2H), 3.06 – 2.73 (m, 1H), 2.46 – 2.35 (m, 1H), 2.28 – 2.16 (m, 2H), 2.14 – 1.99 (m, 1H), 1.17 (t, J = 7.1 Hz, 3H); HRMS (TOF) Calcd for 399.1475, found 399.1470. Purity by HPLC-UV (215 nm) 95% using General Chromatographic Purification Method 2 (retention time = 3.818 min).

*Ethyl 4-(8-chloro-5,6-dihydro-11H-benzo[5,6]cyclohepta[1,2-b]pyridin-11-ylidene)-2,6-dihydroxypiperidine-1-carboxylate (**7**).* Prepared from *Streptomyces setae* ATCC 33774 (0.25 ml stock suspension, contains 20% glycerol) and 13.0 mM solution of **1** (1.0 mL, 13.0 μmol) in DMSO. Yield of **7**: 43 μg, 104 nmol, 0.8%. ^{1}H NMR (600 MHz, DMSO-d_6) δ 8.32 – 8.25 (m,

1H), 8.06 – 7.99 (m, 1H), 7.91 – 7.76 (m, 1H), 7.25 – 7.18 (m, 1H), 7.18 – 7.13 (m, 1H), 7.03 – 6.96 (m, 1H), 5.18 – 5.11 (m, 2H), 4.05 (q, *J* = 7.1 Hz, 2H), 3.79 – 3.66 (m, 2H), 3.21 – 3.05 (m, 2H), 2.34 – 2.12 (m, 4H), 1.18 (t, *J* = 7.2 Hz, 3H); HRMS (TOF) Calcd for 415.1425, found 415.1415. Purity by HPLC-UV (215 nm) 98% using General Chromatographic Purification Method 2 (retention time = 3.700 min).

Synthesis of Analog 8. *Ethyl 4-(8-chloro-5-fluoro-5,6-dihydro-11H-benzo[5,6]cyclohepta[1,2-b]pyridin-11-ylidene)piperidine-1-carboxylate (**8**).* A vented 100 mL jacketed Wheaton reactor equipped with overhead stirrer and Thermo Scientific HAAKE A10 circulating chiller with SC100 immersion circulator was charged with Codexis MicroCyp® lyophile MCYP-P1.2-D07 (135.13 mg, 50.0 nmol: P450 concentration 0.37 nmol/mg), followed by 0.1 M potassium phosphate buffer solution (4.0 mL) at pH 8.0. The reactor was treated with a stock solution of Codexis MCYP-RXN BUFFER (43.5 mL), prepared by dissolving solid MCYP-RXN BUFFER (5.46 g) in de-ionized water (190.0 mL). The reactor was stirred at ambient temperature for 10 minutes and then treated with a solution of **1** (4.79 mg, 12.5 μmol) dissolved in a mixture of DMSO (2 mL) and 0.1 M potassium phosphate buffer solution (0.5 mL) at pH 8.0. The reaction mixture was stirred at 30 ^{o}C for 12 hours, open to the atmosphere. The progress of the reaction was monitored by UPLC-MS. The reaction mixture was quenched by the addition of ethyl acetate (40.0 mL) and centrifuged using an Eppendorf 5810R at 4000 rpm for 10 minutes. The organic layer was removed and passed through a pad of Celite. The aqueous layer was treated with ethyl acetate (40.0 mL) and centrifuged at 4000 rpm for 10 minutes. The layers were allowed to separate and the organic layer was removed and passed through a pad of Celite. The ethyl acetate from the combined organic layers was removed using a rotary evaporator. The crude material was purified using General

Chromatographic Purification Method 2. The dried samples was analyzed by NMR spectroscopy and quantified by external calibration against the ^{1}H NMR spectrum of a 5.0 mM benzoic acid standard solution in DMSO-d_6 using the ERETIC2 function within Topspin V3.2, providing *ethyl 4-(8-chloro-5-hydroxy-5,6-dihydro-11H-benzo[5,6]cyclohepta[1,2-b]pyridin-11-ylidene)piperidine-1-carboxylate (**5**)* as a white solid.[68] Yield of **5**: 1.24 mg, 3.1 μmol, 25%. ^{1}H NMR (600 MHz, DMSO-d_6) δ 8.42 – 8.36 (m, 1H), 7.88 – 7.76 (m, 1H), 7.32 – 7.19 (m, 3H), 7.14 – 7.07 (m, 1H), 6.11 – 5.55 (m, br, 1H), 5.19 – 5.17 (m, 1H), 4.08 – 4.00 (m, 2H), 3.70 – 3.55 (m, 2H), 3.50 – 3.45 (m, 1H), 3.27 – 3.11 (m, 2H), 3.07 – 2.74 (m, 1H), 2.43 – 2.01 (m, 4H), 1.21 – 1.14 (m, 3H); HRMS (TOF) Calcd for 399.1475, found 399.1468. Purity by HPLC-UV (215 nm) 99% using General Chromatographic Purification Method 2 (retention time = 3.910 min).

A 1.5 mL reaction vial equipped with a magnetic stir bar under an atmosphere of nitrogen was treated with **5** (1.24 mg, 3.1 μmol, prepared from MCYP-P1.2-D07) followed by the addition of anhydrous dichloromethane (0.2 mL). The reaction vial was cooled to -78 °C using an acetone dry ice bath, temperature monitored with a J-KEM thermocouple. The clear solution was stirred at -78 °C for 15 minutes and then treated with *N,N*-diethylaminosulfur trifluoride (2.06 μL, 15.6 μmol). The reaction mixture was stirred for 3 hours at -78 °C and the progress of the reaction was monitored by UPLC-MS. The clear solution was quenched by the addition of aqueous 1.0 M $NaHCO_3$ (0.3 mL), transferred to a 1.5 mL Eppendorf tube, vortexed and centrifuged. The layers were allowed to separate and the bottom organic layer was removed. The aqueous layer was extracted with dichloromethane (3 x 0.3 mL) and the combined dichloromethane solvent was removed *in vacuo*. The crude material was purified using General Chromatographic Purification Method 2. Yield of **8**: 25 μg, 62 nmol, 2%. Mixture of conformational isomers.[49] ^{1}H NMR (600 MHz, DMSO-d_6) δ 8.57 – 8.50 (m, 1H), 7.87 – 7.79 (m, 1H), 7.58 – 7.39 (m, 1H), 7.39 – 7.33 (m,

1H), 7.31 – 7.25 (m, 1H), 7.18 – 7.12 (m, 1H), 6.11 – 5.98 (m, 1H), 4.11 – 3.98 (m, 2H), 3.69 – 3.48 (m, 3H), 3.25 – 3.16 (m, 3H), 2.29 – 2.08 (m, 4H), 1.21 – 1.13 (m, 3H); HRMS (TOF) Calcd for 401.1432, found 401.1427. Purity by HPLC-UV (215 nm): Column Waters Atlantis C18 4.6×50 mm, 5 μm; retention time = 2.420 min; peak area 99%; mobile phase A: 0.05% TFA in water (v/v); mobile phase B: 0.05% TFA in acetonitrile (v/v); gradient 95.0% water / 5.0% acetonitrile linear to 5.0% water / 95.0% acetonitrile in 4.0 min, hold at 5.0% water / 95.0% acetonitrile to 5.0 min; flow rate: 2 mL / min; column temperature 60 ^{o}C (retention time = 2.454 min).

Cytochrome P450 BM3 Screen Procedure. Cytochrome P450 BM3 variants were purchased as MicroCyp® lyophiles in bulk quantities from Codexis (Redwood City, CA). Deep well microtiter screening plates were prepared by adding a 5.0 μM stock solution of enzyme (50.0 μL) in 0.1 M potassium phosphate buffer (pH 8.0) to the appropriate well, as indicated in the plate format in Table S5 in the Supporting Information session. Plates were covered with a PlateMax aluminum sealing film (Axygen, Corning, NY) and stored at -80°C until use.

The 96 well BM3 screening plate was thawed to room temperature (23 ^{o}C) and each well was treated with a stock solution of Codexis MCYP-RXN BUFFER (437.5 μL), prepared by dissolving solid MCYP-RXN BUFFER (358 mg) in de-ionized water (25.27 mL). Each well was treated with a 5.0 mM solution of **1** (12.5 μL, 62.5 nmol) in DMSO and the uncovered plate was agitated using an Eppendorf Thermomixer R shaker (300 rpm) at 30 ^{o}C for 12 hours. The reaction was terminated with the addition of acetonitrile (0.5 ml / well), followed by pipet aspiration and mixing using an Eppendorf Thermomixer R (950 rpm) at for 20 minutes. The plate was centrifuged with a Beckman Coulter Allegra instrument at 4000 *g* for 20 minutes and the

supernatant was transferred to a new 96 well plate. The samples were analyzed using the General HPLC-MS Method for Screen Analysis.

Cytochrome P450 BM3 (MicroCyp®) Scale-Up Procedure for the Synthesis of Analogs 9, 10, 11, 12, 13, 14, 15, 16 and 17. A vented 100 mL jacketed Wheaton reactor equipped with overhead stirrer and Thermo Scientific HAAKE A10 circulating chiller with SC100 immersion circulator was charged with MicroCyp® lyophile, followed by 0.1 M potassium phosphate buffer solution (4.0 mL) at pH 8.0. The reactor was treated with a stock solution of MCYP-RXN BUFFER (43.5 mL), prepared by dissolving solid Codexis MCYP-RXN BUFFER (5.46 g) in de-ionized water (190.0 mL). The reactor was stirred at ambient temperature for 10 minutes and then treated with a solution of **1** (4.79 mg, 12.5 μmol) dissolved in a mixture of DMSO (2 mL) and 0.1 M potassium phosphate buffer solution (0.5 mL) at pH 8.0. The reaction mixture was stirred at 30 ^{o}C for 12 hours, open to the atmosphere. The progress of the reaction was monitored by UPLC-MS. The reaction mixture was quenched by the addition of ethyl acetate (40.0 mL) and centrifuged using an Eppendorf 5810R at 4000 rpm for 10 minutes. The organic layer was removed and passed through a pad of Celite. The aqueous layer was treated with ethyl acetate (40.0 mL) and centrifuged at 4000 rpm for 10 minutes. The layers were allowed to separate and the organic layer was removed and passed through a pad of Celite. The ethyl acetate from the combined organic layers was removed using a rotary evaporator. The crude material was purified using General Chromatographic Purification Method 2. The dried samples were analyzed by NMR spectroscopy and quantified by external calibration against the ^{1}H NMR spectrum of a 5.0 mM benzoic acid standard solution in DMSO-d_6 using the ERETIC2 function within Topspin V3.2.

*Ethyl (E)-4-(8-chloro-5,6-dihydro-11H-benzo[5,6]cyclohepta[1,2-b]pyridin-11-ylidene)-3-hydroxypiperidine-1-carboxylate (**9**), ethyl (E)-4-(8-chloro-5-hydroxy-5,6-dihydro-11H-*

benzo[5,6]cyclohepta[1,2-b]pyridin-11-ylidene)-3,4-dihydropyridine-1(2H)-carboxylate ***(10)****, ethyl 4-(8-chloro-3-hydroxy-5,6-dihydro-11H-benzo[5,6]cyclohepta[1,2-b]pyridin-11-ylidene)piperidine-1-carboxylate* ***(11)****, ethyl (Z)-4-(8-chloro-3-hydroxy-5,6-dihydro-11H-benzo[5,6]cyclohepta[1,2-b]pyridin-11-ylidene)-3,4-dihydropyridine-1(2H)-carboxylate* ***(12)****, ethyl (E)-4-(8-chloro-3-hydroxy-5,6-dihydro-11H-benzo[5,6]cyclohepta[1,2-b]pyridin-11-ylidene)-3,4-dihydropyridine-1(2H)-carboxylate* ***(13)****, ethyl (E)-4-(8-chloro-5,6-dihydro-11H-benzo[5,6]cyclohepta[1,2-b]pyridin-11-ylidene)-3,4-dihydropyridine-1(2H)-carboxylate* ***(14)*** *and Ethyl 4-(8-chloro-5,6-dihydro-11H-benzo[5,6]cyclohepta[1,2-b]pyridin-11-ylidene)-3,5-dihydroxypiperidine-1-carboxylate* ***(17)****.* Prepared from MCYP0012 (48.5 mg, 50.0 nmol: P450 concentration 1.03 nmol/mg) and **1** (4.79 mg, 12.5 μmol) dissolved in a mixture of DMSO (2 mL) and 0.1 M potassium phosphate buffer solution (0.5 mL) at pH 8.0. Yield of **9**: 39 μg, 98 nmol. ^{1}H NMR (600 MHz, DMSO-d_6) δ 8.35 (d, J = 4.7 Hz, 1H), 7.64 – 7.54 (m, 1H), 7.41 – 7.04 (m, 4H), 5.38 – 4.82 (m, 1H), 4.42 – 3.86 (m, 7H), 3.38 – 3.24 (m, 2H), 2.89 – 2.73 (m, 2H), 2.58 – 2.12 (m, 2H), 1.20 – 1.10 (m, 3H); HRMS (TOF) Calcd for 399.1475, found 399.1475. Purity by HPLC-UV (210 nm) 95% using General Chromatographic Purification Method 2 (retention time = 4.125 min). Yield of **10**: 16 μg, 40 nmol, 0.3%. ^{1}H NMR (600 MHz, DMSO-d_6) δ 8.46 – 8.37 (m, 1H), 7.89 – 7.77 (m, 1H), 7.50 – 7.21 (m, 3H), 7.21 – 7.11 (m, 1H), 7.00 – 6.83 (m, 1H), 6.06 -5.28 (m, 2H), 5.11 – 4.56 (m, 1H), 4.21 – 4.09 (m, 2H), 3.86 – 2.12 (m, 6H), 1.25 – 1.21 (m, 3H); HRMS (TOF) Calcd for 397.1319, found 397.1312. Purity by HPLC-UV (210 nm) >99% using General Chromatographic Purification Method 2 (retention time = 4.203 min). Yield of **11**: 95 μg, 238 nmol, 2%. ^{1}H NMR (600 MHz, DMSO-d_6) δ 7.90 (d, J = 2.6 Hz, 1H), 7.29 (d, J = 2.3 Hz, 1H), 7.19 (dd, J = 8.1, 2.3 Hz, 1H), 7.05 (d, J = 8.1 Hz, 1H), 6.93 (d, J = 2.7 Hz, 1H), 4.04 (q, J = 7.1 Hz, 2H), 3.65 – 3.55 (m, 2H), 3.37 – 3.11 (m, 4H), 2.83 – 2.68 (m, 2H), 2.36 – 2.29 (m, 1H),

2.28 – 2.21 (m, 1H), 2.21 – 2.10 (m, 2H), 1.17 (t, *J* = 7.1 Hz, 3H); HRMS (TOF) Calcd for 399.1475, found 399.1478. Purity by HPLC-UV (215 nm) 99% using General Chromatographic Purification Method 2 (retention time = 4.077 min). Yield of **12**: 226 μg, 569 nmol, 5%. ^{1}H NMR (600 MHz, DMSO-d_6) δ 7.92 (d, *J* = 2.7 Hz, 1H), 7.29 (d, *J* = 2.3 Hz, 1H), 7.20 (dd, *J* = 8.1, 2.3 Hz, 1H), 7.11 (d, *J* = 8.1 Hz, 1H), 6.95 (d, *J* = 2.7 Hz, 1H), 6.81 (s, 1H), 5.67 (s, 1H), 4.14 (q, *J* = 7.1 Hz, 2H), 3.88 – 3.78 (m, 1H), 3.42 – 3.08 (m, 3H), 2.83 – 2.67 (m, 2H), 2.66 – 2.55 (m, 1H), 2.34 – 2.24 (m, 1H), 1.22 (t, *J* = 7.1 Hz, 3H); HRMS (TOF) Calcd for 397.1319, found 397.1324. Purity by HPLC-UV (215 nm) 97% using General Chromatographic Purification Method 2 (retention time = 4.168 min). Yield of **13**: 8 μg, 20 nmol, 0.2%. ^{1}H NMR (600 MHz, DMSO-d_6) δ 7.94 (d, *J* = 2.7 Hz, 1H), 7.32 (d, *J* = 2.2 Hz, 1H), 7.25 – 7.20 (m, 1H), 7.15 – 7.09 (m, 1H), 6.93 (d, *J* = 2.7 Hz, 1H), 6.84 (d, *J* = 8.2 Hz, 1H), 5.42 (s, 1H), 4.14 (q, *J* = 7.1 Hz, 2H), 3.75 – 3.65 (m, 1H), 3.54 – 3.45 (m, 1H), 3.22 – 3.10 (m, 2H), 2.91 – 2.81 (m, 1H), 2.81 – 2.69 (m, 2H), 2.35 – 2.25 (m, 1H), 1.22 (t, *J* = 7.1 Hz, 3H); HRMS (TOF) Calcd for 397.1319, found 397.1311. Purity by HPLC-UV (215 nm) 96% using General Chromatographic Purification Method 1 (retention time = 6.222 min). Yield of **14**: 15 μg, 39 nmol, 0.3%. ^{1}H NMR (600 MHz, DMSO-d_6) δ 8.37 (d, *J* = 4.7 Hz, 1H), 7.58 (d, *J* = 7.6 Hz, 1H), 7.34 (s, 1H), 7.27 – 7.23 (m, 1H), 7.23 – 7.18 (m, 1H), 7.16 (d, *J* = 8.2 Hz, 1H), 6.90 (s, 1H), 5.54 – 5.35 (m, 1H), 4.14 (q, *J* = 7.1 Hz, 2H), 3.73 – 3.62 (m, 1H), 3.60 – 3.51 (m, 1H), 3.29 – 3.16 (m, 2H), 2.93 – 2.77 (m, 3H), 2.33 – 2.22 (m, 1H), 1.22 (t, *J* = 7.1 Hz, 3H); HRMS (TOF) Calcd for 381.1370, found 381.1368. Purity by HPLC-UV (210 nm) 97% using General Chromatographic Purification Method 1 (retention time = 6.779 min). Yield of **17**: 226 μg, 545 nmol, 4%. ^{1}H NMR (600 MHz, DMSO-d_6) δ 8.40 – 8.35 (m, 1H), 7.64 – 7.62 (m, 1H), 7.43 – 7.25 (m, 3H), 7.07 – 7.05 (m, 1H); 5.57 – 5.11 (m, 2H), 4.65 – 3.92 (m, 6H), 3.44 – 3.08 (m, 4H), 2.98 – 2.77 (m, 2H), 1.22 – 1.12 (m, 3H); HRMS (TOF)

Calcd for 415.1425, found 415.1423. Purity by HPLC-UV (210 nm) >99% using General Chromatographic Purification Method 2 (retention time = 4.413 min).

*Ethyl (Z)-4-(8-chloro-5,6-dihydro-11H-benzo[5,6]cyclohepta[1,2-b]pyridin-11-ylidene)-3,4-dihydropyridine-1(2H)-carboxylate (**15**) and ethyl 4-(8-chloro-11H-benzo[5,6]cyclohepta[1,2-b]pyridin-11-ylidene)piperidine-1-carboxylate (**16**).* Prepared from MCYP0160 (100.0 mg: P450 concentration 2.0 mg/mL) and **1** (4.79 mg, 12.5 μmol) dissolved in a mixture of DMSO (2 mL) and 0.1 M potassium phosphate buffer solution (0.5 mL) at pH 8.0. Yield of **15**: 98 μg, 257 nmol, 2%. ^{1}H NMR (600 MHz, DMSO-d_6) δ 8.37 (dd, J = 4.8, 1.7 Hz, 1H), 7.60 (dd, J = 7.7, 1.7 Hz, 1H), 7.30 (d, J = 2.2 Hz, 1H), 7.24 – 7.19 (m, 2H), 7.15 (d, J = 8.2 Hz, 1H), 6.84 (s, 1H), 5.63 (s, 1H), 4.14 (q, J = 7.1 Hz, 2H), 3.92 – 3.82 (m, 1H), 3.39 – 3.16 (m, 3H), 2.87 – 2.77 (m, 2H), 2.71 – 2.59 (m, 1H), 2.40 – 2.29 (m, 1H), 1.22 (t, J = 7.1 Hz, 3H); HRMS (TOF) Calcd for 381.1370, found 381.1368. Purity by HPLC-UV (288 nm) 97% using General Chromatographic Purification Method 1 (retention time = 6.457 min). Yield of **16**: 20 μg, 53 nmol, 0.4%. ^{1}H NMR (600 MHz, DMSO-d_6) δ 9.32 – 9.21 (m, 2H), 8.18 (d, J = 7.5 Hz, 1H), 8.15 (d, J = 6.6 Hz, 1H), 7.97 (t, J = 7.0 Hz, 1H), 7.55 (s, 1H), 7.40 (d, J = 7.5 Hz, 1H), 7.14 (d, J = 8.3 Hz, 1H), 3.86 – 3.78 (m, 2H), 3.62 – 3.55 (m, 2H), 3.33 – 3.20 (m, 4H), 3.02 – 2.97 (m, 2H), 1.07 (t, J = 7.1 Hz, 3H); HRMS (TOF) Calcd for 381.1370, found 381.1373. Purity by HPLC-UV (210 nm) >99% using General Chromatographic Purification Method 2 (retention time = 3.935 min).

Synthesis of Analogs 18 and 19. *Ethyl 4-(8-chloro-2-(difluoromethyl)-5,6-dihydro-11H-benzo[5,6]cyclohepta[1,2-b]pyridin-11-ylidene)piperidine-1-carboxylate (**18**) and ethyl 4-(8-chloro-4-(difluoromethyl)-5,6-dihydro-11H-benzo[5,6]cyclohepta[1,2-b]pyridin-11-*

*ylidene)piperidine-1-carboxylate (**19**)*. A 1.5 mL reaction vial equipped with a magnetic stir bar under an atmosphere of nitrogen was charged with **1** (20.0 mg, 52.2 μmol) followed by the addition of dimethyl sulfoxide (0.2 mL). At ambient temperature, the clear solution was treated with difluoromethanesulfinate zinc salt (46.3 mg, 156.7 μmol) followed by trifluoroacetic acid (8.0 μL, 104.3 μmol) and 70% aqueous *tert*-butyl hydroperoxide (36.2 μL, 261.0 μmol). The yellow mixture was heat at 50 °C for 15 hours and the progress of the reaction was monitored by UPLC-MS. The reaction mixture was diluted with dimethyl sulfoxide (0.5 mL) and filtered to remove solids. The crude material was purified using General Chromatographic Purification Method 2. Yield of **18**: 1.0 mg, 2.31 μmol, 4%. ^{1}H NMR (400 MHz, Chloroform-*d*) δ 7.62 (d, *J* = 7.9 Hz, 1H), 7.48 (d, *J* = 7.9 Hz, 1H), 7.20 (d, *J* = 2.2 Hz, 1H), 7.19 – 7.16 (m, 2H), 6.62 (t, *J* = 55.6 Hz, 1H), 4.16 (q, *J* = 7.1 Hz, 2H), 3.91 – 3.72 (m, 2H), 3.50 – 3.34 (m, 2H), 3.25 – 3.10 (m, 2H), 3.02 – 2.76 (m, 2H), 2.56 – 2.23 (m, 4H), 1.28 (t, *J* = 7.1 Hz, 3H); HRMS (TOF) Calcd for 433.1494, found 433.1486. Purity by HPLC-UV (288 nm) 96% using General Chromatographic Purification Method 1 (retention time = 8.017 min). Yield of **19**: 1.2 mg, 2.77 μmol, 5%. ^{1}H NMR (400 MHz, Chloroform-*d*) δ 8.71 (d, *J* = 5.4 Hz, 1H), 7.60 (d, *J* = 5.4 Hz, 1H), 7.21 – 7.15 (m, 3H), 6.84 (t, *J* = 54.2 Hz, 1H), 4.17 (q, *J* = 7.1 Hz, 2H), 3.92 – 3.69 (m, 2H), 3.54 – 3.37 (m, 2H), 3.36 – 3.19 (m, 2H), 3.18 – 3.07 (m, 1H), 2.99 – 2.86 (m, 1H), 2.58 – 2.33 (m, 3H), 2.20 – 2.04 (m, 1H), 1.28 (t, *J* = 7.1 Hz, 3H); UPLC-MS *m/z* 433.3 (M+1). HRMS (TOF) Calcd for 433.1494, found 433.1494. Purity by HPLC-UV (288 nm) 95% using General Chromatographic Purification Method 1 (retention time = 7.629 min).

Synthesis of Analog 20. *Ethyl 4-(8-chloro-4-(hydroxymethyl)-5,6-dihydro-11H-*

*benzo[5,6]cyclohepta[1,2-b]pyridin-11-ylidene)piperidine-1-carboxylate (**20**)*. A 1.5 mL reaction vial equipped with a magnetic stir bar under an atmosphere of nitrogen was charged with **1** (10.7 mg, 28.0 μmol) followed by the addition of dimethyl sulfoxide (0.3 mL). At ambient temperature, the clear solution was treated with sodium hydroxymethanesulfinate salt (13.1 mg, 85.0 μmol) followed by trifluoroacetic acid (5.0 μL, 57.7 μmol) and dropwise addition of 70% aqueous *tert*-butyl hydroperoxide (19.6 μL, 141.5 μmol). The yellow mixture was heat at 50 ^{o}C for 2 hours and the progress of the reaction was monitored by UPLC-MS. The crude material was purified using General Chromatographic Purification Method 2. Yield of **20**: 141.3 μg, 342.9 nmol, 1%. ^{1}H NMR (600 MHz, DMSO-d_6) δ 8.33 (d, J = 5.0 Hz, 1H), 7.32 (d, J = 4.9 Hz, 1H), 7.29 (d, J = 2.3 Hz, 1H), 7.21 (dd, J = 8.3, 2.3 Hz, 1H), 7.09 (d, J = 8.1 Hz, 1H), 4.52 (q, J = 15.0 Hz, 2H), 4.05 (q, J = 7.1 Hz, 2H), 3.68 – 3.55 (m, 2H), 3.39 – 3.30 (m, 1H), 3.25 – 3.15 (m, 2H), 3.14 – 3.06 (m, 1H), 2.89 – 2.77 (m, 2H), 2.38 – 2.24 (m, 2H), 2.23 – 2.13 (m, 2H), 1.18 (t, J = 7.1 Hz, 3H); HRMS (TOF) Calcd for 413.1632, found 413.1632. Purity by HPLC-UV (288 nm) 96% General Chromatographic Purification Method 1 (retention time = 4.564 min).

Biomimetic Metalloporphyrin Oxidation (BMO) Screen Procedure. A high throughput BMO screen was completed on a miniature scale, examining the key variables of metalloporphyrin, oxidant and solvent. Nine different metalloporphyrins plus control without metalloporphyrin, six oxidants and two solvents were screened in a matrix of 120 combinations. The remaining variables were held constant according to the standard protocol described below. The reactions were set-up in two 96-well arrays using miniature 8 x 20 mm (0.2 mL) glass vials under standard glove box conditions (H_2O and O_2 <20 ppm).

A 8 x 20 mm (0.2 mL) glass vial equipped with stir bar was dispensed the reaction solvent (100 μL, 4.0 mM) followed by a solution of **1** (5.0 μL, 0.4 μmol), added as a 0.1 M solution in dichloroethane. Stirring was initiated before the metalloporphyrin (4.0 μL, 0.04 μmol) was charged, as a 10.0 mM solution in dichloroethane. The vial was treated with a 0.1 M solution of imidazole (2.4 mL, 0.24 μmol) in H_2O, followed by a 0.4 M solution of formic acid (4.0 μL, 0.16 μmol) in H_2O. Finally, the oxidant (8.0 μL, 0.08 μmol) was added as a 0.1 M solution in dichloroethane. The reaction vial was crimp sealed with a PTFE / Silicone / PTFE septa to the glove box environment before the reaction was left to stir at 25 °C for 18 hours. After this time period, the reaction was diluted with acetonitrile (0.2 mL) and analyzed directly by UPLC/MS. The UPLC/MS method used a 0.1% AcOH / NH_4CO_2H / H_2O gradient over 0.8 minutes, running from 5-95% acetonitrile using a Waters Acquity UPLC BEH C18 30 x 2.1 mm column at 100 °C with a flow rate of 2.5 mL/min and a detection wavelength of 210-360 nm. 0.5 μL injections were made directly from diluted reaction mixtures and ionization monitored in positive mode.

BMO Scale-Up Procedure for the Synthesis of Analogs 21, 22 and 23. *Ethyl 8-chloro-5,6-dihydrodispiro[benzo[5,6]cyclohepta[1,2-b]pyridine-11,2'-oxirane-3',4''-piperidine]-1''-carboxylate (**21**), 8-chloro-1''-(ethoxycarbonyl)-5,6-dihydrodispiro[benzo[5,6]cyclohepta[1,2-b]pyridine-11,2'-oxirane-3',4''-piperidine] 1-oxide (**22**) and 8-chloro-11-(1-(ethoxycarbonyl)piperidin-4-ylidene)-6,11-dihydro-5H-benzo[5,6]cyclohepta[1,2-b]pyridine 1-oxide (**23**)*. A 4-dram glass vail (10 ml) equipped with stir bar was treated with **1** (38.0 mg, 0.1 mmol) followed by a 1:1 solvent mixture of methanol and dichloroethane (10 mL). The reaction mixture was stirred for 5.0 minutes and then treated with *meta*-chloroperoxybenzoic acid (45.0 mg, 0.2 mmol). The reaction vial was screw-cap sealed with a PTFE / Silicone / PTFE septa to the glove box environment before the reaction was left to stir at 25 °C for 18 hours. After this time

period the reaction was diluted with acetonitrile (0.2 mL) and analyzed directly by UPLC/MS. The crude material was purified using General Chromatographic Purification Method 2. Yield of **21**: 380.0 μg, 952.7 nmol, 1%. ^{1}H NMR (600 MHz, DMSO-d_6) δ 8.34 (d, J = 4.7 Hz, 1H), 7.65 (d, J = 7.6 Hz, 1H), 7.36 (d, J = 8.4 Hz, 1H), 7.31 – 7.23 (m, 3H), 4.01 (q, J = 7.1 Hz, 2H), 3.96 – 3.84 (m, 2H), 3.38 – 3.22 (m, 2H), 3.11 – 2.96 (m, 2H), 2.96 – 2.87 (m, 2H), 1.78 – 1.59 (m, 2H), 1.14 (t, J = 7.1 Hz, 3H), 1.02 – 0.79 (m, 2H); HRMS (TOF) Calcd for 399.1475, found 399.1462. Purity by HPLC-UV (215 nm) 99% using General Chromatographic Purification Method 2 (retention time = 4.280 min). Yield of **22**: 1.8 mg, 4.33 μmol, 4%. ^{1}H NMR (600 MHz, DMSO-d_6) δ 8.05 – 8.00 (m, 1H), 7.45 (d, J = 8.4 Hz, 1H), 7.32 – 7.25 (m, 3H), 7.23 – 7.18 (m, 1H), 4.14 – 3.88 (m, 4H), 3.39 – 3.31 (m, 1H), 3.20 – 3.09 (m, 1H), 3.05 – 2.89 (m, 3H), 2.88 – 2.78 (m, 1H), 1.90 – 1.76 (m, 2H), 1.16 (t, J = 7.1 Hz, 3H), 0.87 (d, J = 14.0 Hz, 1H), 0.75 (d, J = 13.4 Hz, 1H); HRMS (TOF) Calcd for 415.1425, found 415.1411. Purity by HPLC-UV (215 nm) 95% using General Chromatographic Purification Method 2 (retention time = 4.290 min). Yield of **23**: 8.35 mg, 20.93 μmol, 21%. ^{1}H NMR (600 MHz, DMSO-d_6) δ 8.13 – 8.07 (m, 1H), 7.27 – 7.18 (m, 4H), 7.14 (d, J = 8.0 Hz, 1H), 4.04 (q, J = 7.1 Hz, 2H), 3.69 – 3.56 (m, 2H), 3.36 – 3.20 (m, 4H), 2.91 – 2.80 (m, 2H), 2.44 – 2.33 (m, 1H), 2.30 – 2.20 (m, 1H), 2.14 – 2.03 (m, 1H), 1.92 – 1.80 (m, 1H), 1.17 (t, J = 7.1 Hz, 3H); HRMS (TOF) Calcd for 399.1475, found 399.1468. Purity by HPLC-UV (215 nm) 95% using General Chromatographic Purification Method 2 (retention time = 4.526 min).

BMO Scale-Up Procedure for the Synthesis of Analog 24. *8-chloro-11-(1-(ethoxycarbonyl)piperidin-4-ylidene)-1-methyl-6,11-dihydro-5H-benzo[5,6]cyclohepta[1,2-b]pyridin-1-ium formate salt (**24**)*. A 4-dram glass vail (10 ml) equipped with stir bar was treated with **1** (38.0 mg, 0.1 mmol) followed by a 1:1 solvent mixture of methanol and dichloroethane (10

mL). The reaction mixture was stirred for 5.0 minutes and then treated with Cu(TDCIPP) (9.5 mg, 0.01 mmol), imidazole (4.0 mg, 0.06 mmol), formic acid (0.015 mL, 0.4 mmol), followed by oxidant cumene hydroperoxide (0.038 mL, 0.2 mmol, 80 wt. percent in H_2O). The reaction vial was screw-cap sealed with a PTFE / Silicone / PTFE septa to the glove box environment before the reaction was left to stir at 25 °C for 18 hours. After this time period the reaction was diluted with acetonitrile (0.2 mL) and analyzed directly by UPLC/MS. The crude material was purified using General Chromatographic Purification Method 2. Yield of **24**: 1.53 mg, 3.45 μmol, 3%. ^{1}H NMR (600 MHz, DMSO-d_6) δ 8.91 (s, 1H), 8.58 (d, J = 7.3 Hz, 1H), 8.10 – 7.95 (m, 1H), 7.37 (d, J = 8.3 Hz, 1H), 7.34 (d, J = 8.1 Hz, 1H), 7.29 (s, 1H), 4.21 (s, 3H), 4.06 (q, J = 7.1 Hz, 2H), 3.86 – 3.77 (m, 1H), 3.77 – 3.67 (m, 1H), 3.52 – 3.36 (m, 2H), 3.27 – 3.01 (m, 3H), 2.98 – 2.85 (m, 1H), 2.48 – 2.41 (m, 1H), 2.41 – 2.34 (m, 1H), 2.29 – 2.19 (m, 1H), 1.96 – 1.86 (m, 1H), 1.19 (t, J = 7.1 Hz, 3H); HRMS (TOF) Calcd for 397.1677, found 397.1670. Purity by HPLC-UV (215 nm) 98% using General Chromatographic Purification Method 2 (retention time = 3.941 min).

Electrochemical Screen and Scale-Up Procedure for the Synthesis of Analog 21 and 25. *Ethyl 8-chloro-5,6-dihydrodispiro[benzo[5,6]cyclohepta[1,2-b]pyridine-11,2'-oxirane-3',4''-piperidine]-1''-carboxylate (**21**) and ethyl 8'-chloro-5-oxo-5',6'-dihydrospiro[azepane-4,11'-benzo[5,6]cyclohepta[1,2-b]pyridine]-1-carboxylate (**25**)*. An undivided electrochemical cell equipped with a magnetic a stir bar was treated with a 0.5 M solution of Et_4NBF_4 (2.0 mL, 1.0 mmol) in acetonitrile followed by H_2O (0.1 mL, 5.5 mmol). The solution was stirred at room temperature for 5.0 minutes and then charged with **1** (19.0 mg, 0.05 mmol). A fitted reticulated vitreous carbon (RVC) anode electrode coupled to a stainless-steel mesh cathode electrode was inserted in to the cell. The mixture was subjected to electrolysis with constant potential (5 V)

across the two electrodes for 1 hour (Figure S1A in the Supporting Information) and the progress of the reaction was monitored by UPLC-MS. The reaction mixture was diluted with dichloromethane (30.0 mL), washed with brine (30.0 mL) and dried over Na_2SO_4. The solution was filtered and concentrated *in vacuo* and the crude material was purified using General Chromatographic Purification Method 3. Yield of **21**: 1.1 mg, 2.76 μmol, 5%. ^{1}H NMR (600 MHz, DMSO-d_6) δ 8.35 (d, J = 4.7 Hz, 1H), 7.65 (d, J = 7.6 Hz, 1H), 7.36 (d, J = 8.3 Hz, 1H), 7.30 – 7.24 (m, 3H), 4.01 (q, J = 7.1 Hz, 2H), 3.97 – 3.83 (m, 2H), 3.38 – 3.22 (m, 2H), 3.11 – 2.96 (m, 2H), 2.95 – 2.88 (m, 2H), 1.80 – 1.56 (m, 2H), 1.15 (t, J = 7.1 Hz, 3H), 1.02 – 0.78 (m, 2H); HRMS (TOF) Calcd for 399.1475, found 399.1467. Purity by HPLC-UV (210 nm) 98% using General Chromatographic Purification Method 3 (retention time = 3.908 min). Yield of **25**: 0.89 mg, 2.23 μmol, 4%. ^{1}H NMR (600 MHz, DMSO-d_6) δ 8.32 (d, J = 4.7 Hz, 1H), 7.52 (d, J = 7.6 Hz, 1H), 7.38 (d, J = 7.9 Hz, 1H), 7.33 (s, 1H), 7.27 – 7.19 (m, 2H), 4.09 – 3.97 (m, 2H), 3.87 – 3.76 (m, 1H), 3.66 – 3.54 (m, 1H), 3.37 – 3.25 (m, 2H), 3.11 – 2.92 (m, 4H), 2.84 – 2.72 (m, 2H), 2.71 – 2.62 (m, 1H), 2.62 – 2.53 (m, 1H), 1.23 – 1.12 (m, 3H); HRMS (TOF) Calcd for 399.1475, found 399.1472. Purity by HPLC-UV (210 nm) 97% using General Chromatographic Purification Method 3 (retention time = 4.425 min).

Note, the electrochemical scale-up procedure also served as the electrochemical screening procedure for loratadine.

Synthesis of Analogs 26 and 27. *Ethyl 4-(8-chloro-7-(trifluoromethyl)-5,6-dihydro-11H-benzo[5,6]cyclohepta[1,2-b]pyridin-11-ylidene)piperidine-1-carboxylate and ethyl 4-(8-chloro-9-(trifluoromethyl)-5,6-dihydro-11H-benzo[5,6]cyclohepta[1,2-b]pyridin-11-ylidene)piperidine-*

*1-carboxylate (**26**, 1:1 mixture of regioisomers) and ethyl 4-(5,6-dihydro-11H-benzo[5,6]cyclohepta[1,2-b]pyridin-11-ylidene)piperidine-1-carboxylate (**27**)*. An undivided electrochemical cell equipped with a magnetic a stir bar was treated with a 0.5 M solution of Et_4NBF_4 (0.4 mL, 0.2 mmol) in dimethyl sulfoxide followed by a 0.5 M solution of H_2SO_4 (0.4 mL, 0.2 mmol) in dimethyl sulfoxide. The solution was stirred at room temperature for 5.0 minutes and then charged with **1** (19.0 mg, 0.05 mmol) and sodium trifluoromethanesulfinate (NaTFMS) salt (39.0 mg, 0.25 mmol). A fitted reticulated vitreous carbon (RVC) anode electrode coupled to a stainless-steel mesh cathode electrode was inserted into the cell. The mixture was subjected to electrolysis with constant potential (5 V) across the two electrodes for 10 hour (Figure S1A and S1B in the Supporting Information) and the progress of the reaction was monitored by UPLC-MS. The reaction mixture was diluted with ethyl acetate (20.0 mL), washed with saturated aqueous $NaHCO_3$ (20.0 mL) and dried over $MgSO_4$. The solution was filtered and concentrated *in vacuo* and the crude material was purified using General Chromatographic Purification Method 3. Yield of **26** as a 1:1 mixture of regioisomers: 83.0 μg, 184.0 nmol, 0.4%. ^{1}H NMR (600 MHz, DMSO-d_6) (regioisomer-1, CF_3 at 7-position) δ 8.40 – 8.35 (m, 1H), 7.55 – 7.49 (m, 2H), 7.37 (d, J = 8.1 Hz, 1H), 7.26 – 7.19 (m, 1H), 4.10 – 4.00 (m, 2H), 3.75 – 3.09 (m, 6H), 3.00 – 2.80 (m, 2H), 2.39 – 2.05 (m, 4H), 1.18 (m, 3H); HRMS (TOF) Calcd for 451.1400, found 451.1388. Purity by HPLC-UV (215 nm) 96% using General Chromatographic Purification Method 3 (retention time = 4.598 min). Yield of **27**: 220.0 μg, 631.4 nmol, 1%. ^{1}H NMR (600 MHz, DMSO-d_6) (regioisomer-2, CF_3 at 9-position) δ 8.40 – 8.35 (m, 1H), 7.65 – 7.60 (m, 2H), 7.46 (s, 1H), 7.26 – 7.19 (m, 1H), 4.10 – 4.00 (m, 2H), 3.75 – 3.09 (m, 6H), 3.00 – 2.80 (m, 2H), 2.39 – 2.05 (m, 4H), 1.18 (m, 3H); HRMS (TOF) Calcd for 349.1916, found 349.1899. Purity by HPLC-UV (215 nm) 95% using General Chromatographic Purification Method 3 (retention time = 4.021 min).

Histamine H_1 Receptor Functional Assay. Compound activity at the human histamine H_1 receptor was determined my measuring receptor-mediated intracellular calcium release using a FLIPR Tetra® system (Molecular Devices, Sunnyvale, CA). Chinese hamster ovary cells stably transfected to express the human histamine H_1 receptor were plated into black clear bottomed 384 well plates (7,500 cells per well) 24 hours prior to the start of the study. The culture media was removed from the wells and was replaced by 80 μL of Hanks' Balanced Salt Solution (HBSS), containing 2-[4-(2-hydroxyethyl)piperazin-1-yl] ethanesulfonic acid (HEPES) (20mM) and Calcium 5 dye as per the manufacturer's directions ((Molecular Devices, Sunnyvale, CA). The plates were incubated at 37 ^oC for 1 hour to allow the dye to load into the cells. Subsequently, the plate was transferred to the FLIPR instrument. Diluted compounds were added to the plate by the FLIPR instrument and the change in fluorescence of each well was measured to determine potential agonist activity. Following an additional 15 minute incubation an EC_{80} concentration of histamine was added to each well to produce an agonist response. Compounds with antagonist activity blocked this response, measured as a change in fluorescence by the FLIPR instrument. IC_{50} values were calculated for each active compound and apparent K_d values were calculated from this IC_{50} value using the Cheng-Prusoff equation.[69] A geometric mean of three replicates were used to determine final human histamine H_1 receptor dissociation constants (K_d).

Human Liver Microsome Stability Assay.[70] Pooled human liver microsomes from Xenotech (Kansas City, KS) at a protein concentration of 0.7 mg/mL were incubated with test compounds (1.0 uM) at 37 ^oC, the total volume was 0.03 mL. A Beckman Coulter Biomek FX (Indianapolis,

IN) 384 well workstation was used for liquid handling and sample incubation. The addition of NADPH was used to initiate the reaction and treatment with ice-cold acetonitrile (75 μL) at the following timepoints (0, 5, 10, 20, 30 and 60 minutes) was utilized to terminate the reaction. The plates containing sample were centrifuged at 3000 rpm for 5 minutes. A total of seven sample wells containing eight test compounds were pooled (i.e. seven test analytes and buspirone as internal standard). An aliquot was removed (45 μL sample / compound) at each timepoint and dried under nitrogen. The samples were reconstituted in 120 μL (0.1% formic acid in water / 0.1% formic acid in acetonitrile, 95:5) and analyzed by LC-MS/MS. A Sciex 5500 TripleQuad (Concord, Ontario, Canada) mass spectrometer was used in line with an Agilent 1290 Infinity Series (Santa Clara, CA) consisting of a LS-1 autosampler and LC pumping system. A standard LC method was used, along with 2 x 20 mm, 2.7 μm, C18 HALO column and flow rate 0.8 mL/min (60 sec cycle time).

Human Hepatocyte Metabolic Stability Assay. Test compounds (0.2 nmol) in DMSO-*d6* were added to a 96 well plate and the solvent was removed *in vacuo*. To each well was added Williams' E medium (0.05 mL) followed by vortex mixing. A suspension of pooled human hepatocytes in Williams' E medium was added to each well to yield a final volume of 0.2 mL at a hepatocyte concentration of 0.5 million cells/mL. The plate was incubated on a rotating shaker at 37 ^{o}C inside a humidified incubator at 90% humidity (95% O_2 / 5% CO_2). At the following timepoints (0, 30, 60, 90, 120 and 240 minutes) aliquots (0.025 mL) were removed and quench with H_2O / acetonitrile (2:1) with 2% formic acid and internal standard naloxone (1.0 μM). The mixtures were centrifuged at 1700 *g* for 5 minutes and the supernatants analyzed by LC-MS/MS. The

regression line must have an $r^2 \geq 0.85$ to report *in vitro* CL_{int} and $T_{1/2}$. Incubation time / *in vitro* $T_{1/2}$ must be ≥0.4 to afford meaningful assessment of liability. Hepatocyte viability as measured by Trypan Blue exclusion (TBE) should not decline >30% during the course of a 4 hour incubation. Equations used to calculate *in vitro* T1/2 and CL_{int}:

$$T_{1/2} = \text{In } 2 / -(\text{slope of In compound signal vs. time plot}) = \text{minutes}$$

$$CL_{int,\ app} = [-\text{slope} / 0.5 \text{ M cells/mL}] \bullet 1000\ \mu\text{L/mL} = \mu\text{L/min/M cells}$$

Apparent Passive Permeability in Ralph Russ Canine Kidney (RRCK) Cell Line Assay.

RRCK apparent passive permeability values were determined using a previously described method.[71]

SFlogD Assay. The shake-flask logD (SFlogD) assay is a method designed to minimize the amount of compound used to determine a molecules octanol-water partition coefficient at pH 7.4, providing a measure of lipophilicity. Liquid handling steps were performed on a Beckman Coulter Biomek FX (Fullerton, CA) using a 96-channel pod. Samples are analyzed using a triple quadrupole mass spectrometer AB Sciex API3000 (Concord, Ontario, Canada) in both positive and negative ion MRM mode.

A solution of 1-octanol (20 mL, 0.13 mol) was treated with a 0.1 M solution of sodium phosphate (2.0 L, 0.2 mol) buffer at pH 7.4, to give Sol-1. The Sol-1 mixture was vigorously shaken and left to stand overnight at room temperature (23 ^{o}C). A solution of 0.1 M sodium phosphate (20 mL, 0.002 mol) buffer at pH 7.4 was treated with 1-octanol (2.0 L, 13.0 mol), to

give Sol-2. The Sol-2 mixture was vigorously shaken and left to stand overnight at room temperature (23 ^{o}C). An internal standard solution was prepared by dissolving CP-628374[72] in acetonitrile, to give Sol-3 at a concentration of 2.5 mg/mL. A 1-octanol internal standard solution was prepared by treating Sol-3 (3.5 mL) with 1:1 methanol / H_2O (1000 mL), to give Sol-4. An internal standard buffer solution was prepared by treating Sol-3 (3.5 mL) with 1-octanol (5.0 mL, 0.032 mol) and 1:1 methanol / H_2O (1000 mL), to give Sol-5. A 10.0 mM stock solution of test compound in DMSO was prepared and 2.0 μL was added to 149.0 μL of Sol-2 in a 96 well plate, followed by the addition of 149.0 μL of Sol-1. The plate was sealed with a silicone well cap-mat and vigorously mixed for 1 hour at 23 ^{o}C using a plate shaker, followed by plate centrifugation at 2500 rpm (1006 x *g*) for 15 minutes. The cap-mat was detached from the plate and an aliquot (4.0 μL) was removed from the 1-octanol phase and transferred into a new 1.0 mL capacity 96 well plate containing Sol-4 (796 μL). In addition, an aliquot (10 μL) from the buffer phase was transferred into the 1.0 mL well capacity plate containing Sol-5 (190 μL). Sample analysis was performed using a triple quadrupole mass spectrometer (AM / Sciex API3000) in both positive and negative ion MRM mode). Samples (2 μL) were injected onto a small cartridge HPLC column using an aqueous isocratic solvent loading, then flushed into the mass spectrometer with an organic elusion solvent. Peak areas were corrected by dilution factors and incorporating the internal standard and the ratio of corrected peak areas were used to calculate the SFlogD.

$$\mathrm{SFlogD}_{\mathrm{oct/buffer}} = \log\left(\frac{[200 - \text{fold dilution of compound}]_{\mathrm{octanol}} \times 200}{[20 - \text{fold compound}]_{\mathrm{buffer}} \times 20}\right)$$

ASSOCIATED CONTENT

Supporting Information Available

The Supporting Information is available free of charge on the ACS Publication website ACS Publication website at DOI: *(insert DOI link)*.

Lead diversification screening panels, HPLC-MS screening results, cyclic voltammetry reading, protein-ligand docking protocols and ^{1}H NMR, COSY, HSQC, HMBC, NOE spectra of intermediates and final products *(insert link to Supporting Information PDF)*.

Molecular Formula Strings *(insert link to CSV)*.

AUTHOR INFORMATION

Corresponding Author

*E-Mail**:** manjinder.lall@pfizer.com

Notes

The authors declare no competing financial interest.

ACKNOWLEDGMENT

We gratefully acknowledge the extended Monobactam Team for collaborative efforts and helpful discussions. In particular, we are indebted to Michael A. Brodney, Adam M. Gilbert and Mark C. Noe for helpful discussions regarding this work. For their technical expertise, we extend our gratitude to Ben Burke, Anthony A. Carlo, Laurence Philippe, Raman Sharma, Mark A. West,

Kim Wilson, Hui Zhang, Gilles H. Goetz and James J. Federico. We thank Matthew F. Brown for manuscript review and providing useful feedback.

NON-STANDARD ABBREVIATIONS USED

ATCC, American Type Culture Collection; BMO, biomimetic metalloporphyrin oxidation; BM3, *Bacillus megaterium* CYP102A1; CHP, cumene hydroperoxide; ECTFM, electrochemical trifluoromethylation; ERETIC2, electronic reference to access in vivo concentrations 2; H_1 receptor, human histamine H_1 receptor; HHEP *CLint*, human hepatocyte intrinsic clearance CL_{int} (μL/min/million cells); HLM *CLint*, human liver microsome intrinsic clearance CL_{int} (μL/min/mg); LipE, lipophilic efficiency; LM, liver microsomes; LSF, late stage functionalization; LSLD, late stage lead diversification; M+/-number, average mass change difference between parent and analog (i.e. delta mass); Met ID, metabolite identification; Oxone, potassium peroxymonosulfate; P450 BM3, cytochrome P450 from *Bacillus megaterium* CYP102A1; PhIO, iodosobenzene; rhCYP, recombinant cytochrome P450; RRCK P_{app}, apparent passive permeability in the Ralph Russ Canine Kidney cell line P_{app} (10^{-6} cm/sec); RVC, reticulated vitreous carbon; SFlogD, Shake-flask logarithm of distribution coefficient

REFERENCES

1. a) Fessner, N. D. P450 Monooxygenases Enable Rapid Late-Stage Diversification of Natural Products *via* C−H Bond Activation. *ChemCatChem* **2019**, *11*, 2226-2242. b) Scott Obach, R.; Walker, G. S.; Sharma, R.; Jenkinson, S.; Tran, T. P.; Stepan, A. F. Lead

Diversification at the Nanomole Scale Using Liver Microsomes and Quantitative Nuclear Magnetic Resonance Spectroscopy: Application to Phosphodiesterase 2 Inhibitors. *J. Med. Chem.* **2018**, *61*, 3626-3640. c) Stepan, A. F.; Tran, T. P.; Helal, C. J.; Brown, M. S.; Chang, C.; O'Connor, R. E.; De Vivo, M.; Doran, S. D.; Fisher, E. L.; Jenkinson, S.; Karanian, D.; Kormos, B. L.; Sharma, R.; Walker, G. S.; Wright, A. S.; Yamg, E. X.; Brodney, M. A.; Wager, T. T.; Verhoest, P. R.; Scott Obach, R. Late-Stage Microsomal Oxidation Reduces Drug–Drug Interaction and Identifies Phosphodiesterase 2A Inhibitor PF-06815189. *ACS Med. Chem. Lett.* **2018**, *9*, 68-72. d) Brodney, M. A.; Sharma, R.; Lazzaro, J. T.; Walker, G. S.; Scott Obach, R. Harnessing Biosynthesis and Quantitative NMR for Late Stage Functionalization of Lead Molecules: Application to the M1 Positive Allosteric Modulator (PAM) Program. *Bioorg. Med. Chem. Lett.* **2018**, *28*, 2068-2073.

2. Cernak, T.; Dykstra, K. D.; Tyagarajan, S.; Vachal, P.; Krska, S. W. The Medicinal Chemist's Toolbox for Late Stage Functionalization of Drug-Like Molecules. *Chem. Soc. Rev.* **2016**, *45*, 546-576.
3. Gesmundo, N. J.; Sauvagnat, B.; Curran, P. J.; Richards, M. P.; Andrews, C. L. Dandiker, P. J.; Cernak, T. Nanoscale Synthesis and Affinity Ranking. *Nature* **2018**, *557*, 228-232.
4. a) Dobson, C. D. Chemical Space and Biology. *Nature* **2004**, *432*, 824-828. b) Ertl, P. Cheminformatics Analysis of Organic Substituents: Identification of the Most Common Substituents, Calculation of Substituent Properties, and Automatic Identification of Drug-like Bioisosteric Groups. *J. Chem. Inf. Comput. Sci.* **2003**, *43*, 374-380. c) Lipinski, C. A.; Lombardo, F.; Dominy, B. W.; Feeney, P. J. Experimental and Computational Approaches to Estimate Solubility and Permeability in Drug Discovery and Development Settings. *Adv. Drug Deliv. Rev.* **1997**, *23*, 3-25.

5. a) Burke, M. D.; Schreiber, S. L. A Planning Strategy for Diversity-Oriented Synthesis. *Angew. Chem. Int. Ed.* **2004**, *43*, 46-58. b) Spring, D. R. Diversity-Oriented Synthesis; A Challenge for Synthetic Chemists. *Org. Biomol. Chem.* **2003**, *1*, 3867-3870.
6. Johnson, T. W.; Gallego, R. A.; Edwards, M. P. Lipophilic Efficiency as an Important Metric in Drug Design. *J. Med. Chem.* **2018**, *61*, 6401-6420.
7. a) Galloway, W. R. J. D.; Isidro-Llobet, A.; Spring, D. R. Diversity-Oriented Synthesis as a Tool for the Discovery of Novel Biologically Active Small Molecules. *Nat. Commun.* **2010**, *80*, 1-13. b) Galloway, W. R. J. D.; Spring, D. R. Is Synthesis the Main Hurdle for the Generation of Diversity in Compound Libraries for Screening? *Expert Opin. Drug Discovery* **2009**, *4*, 467-472.
8. a) Bostrom, J.; Brown, D. G.; Young, R. J.; Keseru, G. M. Expanding the Medicinal Chemistry Synthetic Toolbox. *Nature Reviews Drug Discovery*, **2018**, *17*, 709-727. b) Blakemore, D. C.; Castro, L.; Churcher, I.; Rees, D. C.; Thomas, A. W.; Wilson, D. M.; Wood, A. Organic Synthesis Provides Opportunities to Transform Drug Discovery. *Nature Chemistry* **2018**, *10*, 383-394.
9. a) Waring, M. J.; Arrowsmith, J.; Leach, A. R.; Leeson, P. D.; Mandrell, S.; Owen, R. M.; Pairaudeau, G.; Pennie, W. D.; Pickett, S. D.; Wang, J.; Wallace, O.; Weir, A. An Analysis of the Attrition of Drug Candidates from Four Major Pharmaceutical Companies. *Nat. Rev. Drug Discov.* **2015**, *14*, 475-486. b) Meanwell, N. A. Improving Drug Candidates by Design: A Focus on Physicochemical Properties as a Means of Improving Compound Disposition and Safety. *Chem. Res. Toxicol.* **2011**, *24*, 1420-1456.
10. a) Scott Obach, R.; Walker, G. S.; Brodney, M. A. Biosynthesis of Fluorinated Analogs of Drugs Using Human Cytochrome P450 Enzymes Followed by Deoxyfluorination and

Quantitative Nuclear Magnetic Resonance Spectroscopy to Improve Metabolic Stability. *Drug Metab. Dispos.* **2016**, *44*, 634-646. b) Walker, G. S.; Bauman, J. N.; Ryder, T. F.; Smith, E. B.; Spracklin, D. K.; Scott Obach, R. Biosynthesis of Drug Metabolites and Quantitation Using NMR Spectroscopy for Use in Pharmacologic and Drug Metabolism Studies. *Drug Metab. Dispos.* **2014**, *42*, 1627-1639.

11. Bertrand, S.; Bohni, N.; Schnee, S.; Schumpp, O.; Gindro, K.; Wolfender, J.-L. Metabolite Induction via Microorganism Co-Culture: A Potential Way to Enhance Chemical Diversity for Drug Discovery. *Biotechnol. Adv.* **2014**, *32*, 1180-1204.
12. Sawayama, A. M.; Chen, M. M. Y.; Kulanthaivel; P.; Kuo, M.-S.; Hemmerle, H.; Arnold, F. H. A Panel of Cytochrome P450 BM3 Variants To Produce Drug Metabolites and Diversify Lead Compounds. *Chem. Eur. J.* **2009**, *15*, 11723-11729.
13. Pereira, M. M.; Dias, L. D.; Calvete, M. J. F. Metalloporphyrins: Bioinspired Oxidation Catalysts. *ACS Catal.* **2018**, *8*, 10784-10808.
14. a) Yan, M.; Kawamata, Y.; Baran, P. S. Synthetic Organic Electrochemical Methods Since 2000: On the Verge of a Renaissance. *Chem. Rev.* **2017**, *117*, 13230-13319. b) Mandic, Z. Electrochemical Methods in Drug Discovery and Development. *Bulg. Chem. Commun.* **2017**, *49*, 65-73.
15. Duncton, M. A. J. Minisci Reactions: Versatile CH-Functionalizations for Medicinal Chemists. *Med. Chem. Commun.* **2011**, *2*, 1135-1161.
16. Smith, J. M.; Dixon, J. A.; deGruyter, J. N.; Baran, P. S. Alkyl Sulfinates: Radical Precursors Enabling Drug Discovery**.** *J. Med. Chem.* **2019**, *62*, 2256-2264.
17. McAtee, R. C.; McClain, E. J.; Stephenson, C. R. J. Illuminating Photoredox Catalysis. *Trends in Chemistry* **2019**, *1*, 111-125.

18. Tenn, M. W.; Steacy, L. M.; Ng, C. C.; Ellis, A. K. Onset of Action for Loratadine Tablets for the Symptomatic Control of Seasonal Allergic Rhinitis in Adults Challenged with Ragweed Pollen in the Environmental Exposure Unit: A Post Hoc Analysis of Total Symptom Score. *Allergy Asthma Clin. Immunol.* **2018**, *14*, 5/1-5/7.

19. a) Schumacher, D. P.; Murphy, B. L.; Clark, J. E.; Tahbaz, P.; Mann, T. A. Superacid Cyclodehydration of Ketones in the Production of Tricyclic Antihistamines. *J. Org. Chem.* **1989**, *54*, 2242-2244. b) Doran, H. J.; O'Neill, P. M. Process for Preparing Tricyclic Compounds Having Antihistaminic Activity. PCT Int. Appl., 2000037457, Jun 29, 2000. c) Cuboni, S.; Devigny, C.; Hoogeland, B.; Strasser, A.; Pomplun, S.; Hauger, B.; Hofner, G.; Wanner, K. T.; Eder, M.; Buschauer, A.; Holsboer, F.; Hausch, F. Loratadine and Analogues: Discovery and Preliminary Structure–Activity Relationship of Inhibitors of the Amino Acid Transporter B^0AT2. *J. Med. Chem.* **2014**, *57*, 9473-9479. d) Wang, Y.; Wang, J.; Lin, Y.; Si-Ma, L.-F.; Wang, D.-H.; Chen, L.-G.; Liu, D.-K. Synthesis and Antihistamine Evaluations of Novel Loratadine Analogues. *Bioorg. Med. Chem. Lett.* **2011**, *21*, 4454-4456. e) Randall, K. L.; Hawkins, C. A. Antihistamines and Allergy. *Aust. Prescr.* **2018**, *41*, 41-45. f) Church, M. K.; Church, D. S. Pharmacology of Antihistamines. *Indian J. Dermatol.* **2013**, *58*, 219-224. g) Anthes, J. C.; Gilchrest, H.; Richard, C.; Eckel, S.; Hesk, D.; West, R. E., Jr.; Williams, S. M.; Greenfeder, S.; Billah, M.; Kreutner, W.; Egan, R. W. Biochemical Characterization of Desloratadine, a Potent Antagonist of the Human Histamine H(1) Receptor. *Eur. J. Pharmacol.* **2002**, *449*, 229-237.

20. Bernhardt, R. *J.* Cytochromes P450 as Versatile Biocatalysts. *Biotechnology* **2006**, *124*, 128-145.

21. a) Kang, M. J.; Song, W. H.; Shim, B. H.; Oh, S. Y.; Lee, H. Y.; Chung, E. Y.; Sohn, Y.; Lee, J. Pharmacologically Active Metabolites of Currently Marketed Drugs: Potential Resources for New Drug Discovery and Development. *Yakugaku Zasshi* **2010**, *130*, 1325-1337. b) Miao, Z.; Obach, R. S. Alcohols and Phenols: Absorption, Distribution, Metabolism and Excretion. In *Metabolism, Pharmacokinetics and Toxicity of Functional Groups: Impact of Chemical Building Blocks on ADMET*, David, T. Ed.; The Royal Society of Chemistry: Cambridge, UK, 2010; Chapter 10, pp 460-485.

22. a) Mao, F.; Ni, W.; Xu, X.; Wang, H.; Wang, J.; Ji, M.; Li, J. Chemical Structure-Related Drug-Like Criteria of Global Approved Drugs. *Molecules* **2016**, *21*(1), 75/1-75/18. b) Henkel, T.; Brunne, R. M.; Muller, H.; Reichel, F. Statistical Investigation into the Structural Complementarity of Natural Products and Synthetic Compounds. *Angew. Chem. Int. Ed.* **1999**, *38*, 643-647. c) Trader, D. J.; Carlson, E. E. Chemoselective Hydroxyl Group Transformation: An Elusive Target. *Mol. Biosystems* **2012**, *8*, 2484-2493.

23. Ghosal, A.; Gupta, S.; Ramanathan, R.; Yuan, Y.; Lu, X.; Su, A. D.; Alvarez, N.; Zbaida, S.; Chowdhury, S. K.; Alton, K. B. Metabolism of Loratadine and Further Characterization of its In Vitro Metabolites. *Drug Metab. Lett.* **2009**, *3*, 162-170.

24. Zhu, M.; Zhang, H.; Humphreys, W. G. Drug Metabolite Profiling and Identification by High-Resolution Mass Spectrometry. *J. Biol. Chem.* **2011**, *286*, 25419-25425.

25. a) Gehlhaar, D. K.; Verkhivker, G. M.; Rejto, P. A.; Sherman, C. J.; Fogel, D. B.; Fogel, L. J.; Freer, S. T. Molecular Recognition of the Inhibitor AG-1343 by HIV-1 Protease: Conformationally Flexible Docking by Evolutionary Programming. *Cell Chem. Biol.* **1995**, *2*, 317-324. b) Marrone, T. J.; Luty, B. A.; Rose, P. W. Discovering High-Affinity Ligands from the Computationally Predicted Structures and Affinities of Small Molecules

Bound to a Target: A Virtual Screening Approach. *Perspect. Drug Discovery Des.* **2000**, *20*, 209-230. c) Polak, E.; Ribiere, G. "Note sur la Convergence de Methodes de Directions Conjuguees. Revue Francaise Inf. Rech. Oper., Serie Rouge" 1969, 16-R1, 35. d) Mohamadi, F., Richards, N. G. J.; Guida, W. C.; Liskamp, R.; Lipton, M.; Caufield, C.; Chang, G.; Hendrickson, T.; Still, W. C. Macromodel—An Integrated Software System for Modeling Organic and Bioorganic Molecules Using Molecular Mechanics. *J. Comput. Chem.* **1990**, *11*, 440-467.

26. a) Sjogren, E.; Lennernas, H.; Anderson, T. B.; Grasjo, J.; Bredberg, U. The Multiple Depletion Curves Method Provides Accurate Estimates of Intrinsic Clearance (CLint), Maximum Velocity of the Metabolic Reaction (Vmax), and Michaelis Constant (Km): Accuracy and Robustness Evaluated Through Experimental Data and Monte Carlo Simulations. *Drug Metab. Dispos.* **2009**, *37*, 47-58. b) Nassar, A.-E.; Kamel, A. M.; Clarimont, C. Improving the Decision-Making Process in the Structural Modification of Drug Candidates: Enhancing Metabolic Stability. *Drug Discov. Today* **2004**, *9*, 1020-1028.
27. a) Demain, A. L. Importance of Microbial Natural Products and the Need to Revitalize Their Discovery. *J. Ind. Microbiol. Biotechnol.* **2014**, *41*, 185-201. b) Cragg, G. M.; Newman, D. J. Natural Products: A Continuing Source of Novel Drug Leads. *Biochimica et Biophysica Acta* **2013**, *1830*, 3670-3695.
28. Hypha Discovery Ltd. Lead Compound Diversification and Late Stage Functionalization. https://www.hyphadiscovery.co.uk/our-services/lead-diversification/ (accessed May 19, 2019).
29. a) Bianchini, L. F.; Arruda, M. F. C.; Vieira, S. R.; Campelo, P. M. S.; Gregio, A. M. T.; Rosa, E. A. R. Microbial Biotransformation to Obtain New Antifungals. *Front. Microbiol.*

2015, *6*, 1-12. b) Hegazy, M.-E. F.; Mohamad, T. A.; El Shamy, A. I.; Mohamad, A.-E.-H. H.; Mahalel, U. A.; Reda, E. H.; Shaheen, A. M.; Tawfik, W. A.; Shahat, A. A.; Shams, K. A.; Abdel-Azim, N. S.; Hammouda, F. H. Microbial Biotransformation as a Tool for Drug Development Based on Natural Products From Mevalonic Acid Pathway: A Review. *J. Adv. Res.* **2014**, *6*, 17-33. c) Restaino, O. F.; Marseglia, M.; De Castro, C.; Diana, P.; Forni, P.; Parrilli, M.; De Rosa, M.; Schiraldi, C. Biotechnological Transformation of Hydrocortisone to 16α-Hydroxy Hydrocortisone by Streptomyces roseochromogenes. *Appl. Microbiol. Biotechnol.* **2014**, *98*, 1291-1299.

30. a) Product *m/z* 413c (M+30) is observed in well 28 generated from *Streptomyces setae* ATCC 33774, not shown in Figure 6. b) Borges, K. B.; Borges, W. S.; Duran-Patron, R.; Pupo, M. T.; Bonato, P. S.; Collado, I. G. Stereoselective Biotransformations Using Fungi as Biocatalysts. *Tetrahedron: Asymmetry* **2009** *20*, 385-397.
31. Manikandan, P.; Nagini, S. Cytochrome P450 Structure, Function and Clinical Significance: A Review. *Curr. Drug Targets* **2018**, *19*, 38-54.
32. Directed Evolution of Enzymes and Binding Proteins. https://www.nobelprize.org/uploads/2018/10/advanced-chemistryprize-2018.pdf (accessed May 24, 2019).
33. a) Arnold, F. H. Directed Evolution: Bringing New Chemistry to Life. *Angew. Chem. Int. Ed.* **2018**, *57*, 4143-4148. b) Behrendorff, J. B. Y. H.; Huang, W.; Gillam, E. M. J. Directed Evolution of Cytochrome P450 Enzymes for Biocatalysis: Exploiting the Catalytic Versatility of Enzymes with Relaxed Substrate Specificity. *Biochem. J.* **2015**, *467*, 1-15. c) Heel, T.; McIntosh, J. A.; Dodani, S. C.; Meyerowitz, J. T.; Arnold, F. H. Non-Natural Olefin Cyclopropanation Catalyzed by Diverse Cytochrome P450s and Other

Hemoproteins. *ChemBioChem* **2014**, *15*, 2556-2562. d) Kumar, S. Engineering Cytochrome P450 Biocatalysts for Biotechnology, Medicine and Bioremediation. *Expert Opin. Drug. Metab. Toxicol.* **2010**, *6*, 115-131. e) Rentmeister, A.; Arnold, F. H.; Fasan, R. Chemo-Enzymatic Fluorination of Unactivated Organic Compounds. *Nat. Chem. Biol.* **2009**, *5*, 26-28. f) Lamb, D. C.; Waterman, M. R.; Kelly, S. L.; Guengerich, F. P. Cytochromes P450 and Drug Discovery. *Curr. Opin. Biotechnol.* **2007**, *18*, 504-512.

34. a) Jeffreys, L. N.; Poddar, H.; Golovanova, M.; Levy, C. W.; Girvan, H. M.; McLean, K. J.; Voice, M. W.; Leys, D.; Munro, A. W. Novel Insights into P450 BM3 Interactions with FDA-Approved Antifungal Azole Drugs. *Scientific Reports* **2019**, *9(1)*, 1577. b) Lewis, J. C.; Arnold, F. H. Catalysts on Demand: Selective Oxidations by Laboratory-Evolved Cytochrome P450 BM3. *Chimia* **2009**, *63*, 309-312. c) Otey, C. R.; Bandara, G.; Lalonde, J.; Takahashi, K.; Arnold, F. H. Preparation of Human Metabolites of Propranolol Using Laboratory-Evolved Bacterial Cytochromes P450. *Biotechnol. Bioeng.* **2006**, *93*, 494-499.
35. a) Di Nardo, G.; Gilardi, G. Optimization of the Bacterial Cytochrome P450 BM3 System for the Production of Human Drug Metabolites. *Int. J. Mol. Sci.* **2012**, *13*, 15901-15924. b) Dong, J.; Fernandez-Fueyo, E.; Hollmann, F.; Paul, C. E.; Pesic, M.; Schmidt, S.; Wang, Y.; Younes, S.; Zhang, W. Biocatalytic Oxidation Reactions: A Chemist's Perspective. *Angew. Chem. Int. Ed.* **2018**, *57*, 9238-9261.
36. Kaluzna, I.; Schmitges, T.; Straatman, H.; van Tegelen, D.; Muller, M.; Schurmann, M.; Mink, D. Enabling Selective and Sustainable P450 Oxygenation Technology. Production of 4-Hydroxy-α-isophorone on Kilogram Scale. *Org. Process Res. Dev.* **2016**, *20*, 814-819.
37. Codexis Screening Kits and Biocatalysts. https://www.codexis.com/products/screening-kits/ (accessed May 25, 2019).

38. Ellsworth, B. A.; Wang, Y.; Zhu, Y.; Pendri, A.; Gerritz, S. W.; Sun, C.; Carlson, K. E.; Kang, L.; Baska, R. A.; Yang, Y.; Huang, Q.; Burford, N. T.; Cullen, M. J.; Johnghar, S.; Behnia, K.; Pelleymounter, M. A.; Washburn, W. N.; Ewing, W. R. Discovery of Pyrazine Carboxamide CB1 Antagonists: The Introduction of a Hydroxyl Group Improves the Pharmaceutical Properties and In Vivo Efficacy of the Series. *Bioorg. Med. Chem. Lett.* **2007**, *17*, 3978-3982.

39. a) Mandic, Z. Naranda, A.; Novak, P.; Brajsa, K.; Derek, M.; Ivekovic, D. New Derivatives of Tylosin: Chemical and Electrochemical Oxidation Products of Desmycosin. *J. Antibiot.* **2002**, *55*, 807-813. b) Mandic, Z. Naranda, A.; Lopotar, N.; Duic, L.; Ivekovic, D.; Tkalcec, M. Tylosin Derivatives. *J. Antibiot.* **1999**, *52*, 1143-1145.

40. Jurva, U.; Weidolf, L. Electrochemical Generation of Drug Metabolites with Applications in Drug Discovery and Development. *Trends Anal. Chem.* **2015**, *70*, 92-99.

41. a) Fodi, T.; Ignacz, G.; Decsi, B.; Beni, Z.; Turos, G. I.; Kupai, J.; Weiser, D. B.; Greiner, I.; Huszthy, P.; Balogh, G. T. Biomimetic Synthesis of Drug Metabolites in Batch and Continuous-Flow Reactors. *Chem. Eur. J.* **2018**, *24*, 9385-9392. b) Baglia, R. A.; Zaragoza, J. P. T.; Goldberg, D. P. Biomimetic Reactivity of Oxygen-Derived Manganese and Iron Porphyrinoid Complexes**.** *Chem. Rev.* **2017**, *117*, 13320-13352. c) Che, C.-M.; Lo, V. K.-Y.; Zhou, C.-Y.; Huang, J.-S. Selective Functionalisation of Saturated C–H Bonds with Metalloporphyrincatalysts. *Chem. Soc. Rev.* **2011**, *40*, 1950-1975.

42. a) Masood, M. A.; Farrant, E.; Morao, I.; Bazin, M.; Perez, M.; Bunnage, M. E.; Fancy, S.-A.; Peakman, T. Lead Diversification. Application to Existing Drug Molecules: Mifepristone 1 and Antalarmin 8. *Bioorg. Med. Chem. Lett.* **2012**, *22*, 723-728. b) Masood, M. A.; Bazin, M.; Bunnage, M. E.; Calabrese, A.; Cox, M.; Fancy, S.-A.; Farrant, E.;

Pearce, D. W.; Perez, M.; Hitzel, L.; Peakman, T. Lead Diversification 2: Application to P38, gMTP and Lead Compounds. *Bioorg. Med. Chem. Lett.* **2012**, *22*, 1255-1262.

43. Murahashi, S. I.; Noji, S.; Hirabayashia, T.; Komiya, N. Manganese-Catalyzed Enantioselective Oxidation of C–H Bonds of Alkanes and Silyl Ethers to Optically Active Ketones. *Tetrahedron: Asymmetry* **2005**, *16*, 3527-3535.
44. Bernadou, J.; Meunier, B. Biomimetic Chemical Catalysts in the Oxidative Activation of Drugs. *Adv. Synth. Catal.* **2004**, *346*, 171-184.
45. Frontier Scientific. http://www.frontiersci.com/ (accessed Jul 2, 2019).
46. Product (*m/z* 413c (M+32) was also observed by HPLC-MS in the BM3 screen by variants MCYP0012, MCYP0036, MCYP0052, MCYP0057 and MCYP-P1.2-A07.
47. TCI 1.7 mm MicroCryoProbe. https://www.bruker.com/products/mr/nmr/probes/cryoprobes/micro-cryoprobe/overview.html (accessed Aug 7, 2019).
48. Hong, R. S.; Hwang, K. H.; Kim, S.; Cho, H. E.; Lee, H. J.; Hong, J. T.; Moon, D. C. Survey of ERETIC2 NMR for Quantification. *Journal of the Korean Magnetic Resonance Society* **2013**, *17*, 98-104.
49. Piwinski, J. J.; Wong, J. K.; Chan, T.-M.; Green, M. J.; Ganguly, A. K. Hydroxylated Metabolites of Loratadine: An Example of Conformational Diastereomers Due to Atropisomerism. *J. Org. Chem.* **1990**, *55*, 3341-3350.
50. St. Jean, D. J. Jr.; Fotsch, C. Mitigating Heterocycle Metabolism in Drug Discovery. *J. Med. Chem.* **2012**, *55*, 6002-6020.

51. Ramanathan, R. Reyderman, L.; Kulmatycki, K.; Su, A.-D.; Alvarez, N.; Chowdhury, S. K.; Alton, K. B.; Wirth, M. A.; Clement, R. P.; Statkevich, P.; Patrick, J. E. Disposition of Loratadine in Healthy Volunteers. *Xenobiotica*, **2007**, *37*, 753-769.

52. a) See, S. Desloratadine for Allergic Rhinitis. *Am. Fam. Physician* **2003**, *68*, 2015-2016. b) Simon, F. E. R.; Prenner, B. M.; Fin, A. Jr. Efficacy and Safety of Desloratadine in the Treatment of Perennial Allergic Rhinitis. *J. Allergy Clin. Immunol.* **2003**, *111*, 617-622.

53. Robertson, A.; Francis, J. E.; Witkop, B. Rearrangements of Dehydroproline Derivatives. *J. Am. Chem. Soc.* **1962**, *84*, 1709-1715.

54. Stereo-configuration of analog **7** in Figure 9 is represented by ethyl (2*R*,6*S*,*E*)-4-(8-chloro-5,6-dihydro-11H-benzo[5,6]cyclohepta[1,2-b]pyridin-11-ylidene)-2,6-dihydroxypiperidine-1-carboxylate. The other hydroxyl stereoisomers of analog **7** were docked against CYP2D6 and show similar out-of-range protein-ligand docks as in Figure 9, placing the methylene hydrogen of the ethyl carbamate portion of the molecule >13 Å from the iron(IV)-oxo porphyrin radical cation in the CYP active site.

55. Fauq, A. H. "*N,N*-Diethylaminosulfur Trifluoride" In *Encyclopedia of Reagents for Organic Synthesis*, Paquette, L. A. Eds.; John Wiley & Sons: New York, 1995: Volume 3, pp 1787-1790.

56. Shah, P.; Westwell, A. D. The Role of Fluorine in Medicinal Chemistry. *J. Enzyme Inhib. Med. Chem.* **2007**, *22*, 527-540.

57. Wang, J.; Sanchez-Rosello, M.; Acens, J. L.; Del Pozo, C.; Sorochinsky, A. E.; Fustero, S.; Soloshonok, V. A.; Liu, H. Fluorine in Pharmaceutical Industry: Fluorine-Containing Drugs Introduced to the Market in the Last Decade (2001–2011). *Chem. Rev.* **2014**, *114*, 2432-2506.

58. Baran Diversinates. https://www.sigmaaldrich.com/chemistry/chemistry-products.html?TablePage=113932507 (accessed Aug 26, 2019).

59. Meanwell, N. A. Synopsis of Some Recent Tactical Application of Bioisosteres in Drug Design. *J. Med. Chem.* **2011**, *54*, 2529-2591.

60. a) DiRocco, D. A.; Dykstra, K.; Krska, S.; Vachal, P.; Conway, D. V.; Tudge, M. Late-Stage Functionalization of Biologically Active Heterocycles Through Photoredox Catalysis. *Angew. Chem. Int. Ed.* **2014**, *53*, 4802-4806. b) Hill, C. L. Introduction of Functionality into Unactivated Carbon-Hydrogen Bonds. Catalytic Generation and Nonconventional Utilization of Organic Radicals. *Synlett*, **1995**, 127-132.

61. a) Beatty, J. W.; Douglas, J. J.; Cole, K. P.; Stephenson, C. R. J. A Scalable and Operationally Simple Radical Trifluoromethylation. *Nat. Commun.* **2015**, *6*, 7919. b) Sun, A. C.; McClain, E. J.; Beatty, J. W.; Stephenson, C. R. J. Visible Light-Mediated Decarboxylative Alkylation of Pharmaceutically Relevant Heterocycles. *Org. Lett.* **2018**, *20*, 3487-3490.

62. Halperin, S. D.; Fan, H.; Chang, S.; Martin, R. E.; Britton, R. A Convenient Photocatalytic Fluorination of Unactivated C–H Bonds. *Angew. Chem. Int. Ed.* **2014**, *53*, 4690-4693.

63. a) Two control reactions were run without metalloporphyrin catalyst Cu(TDCIPP), one with cumene hydroperoxide oxidant (2.0 eq.) and one with *meta*-chloroperoxybenzoic acid oxidant (2.0 eq.). The two control reactions gave matching product profiles, however product conversion was superior with *m*CPBA. Therefore, the *m*CPBA control reaction was submitted for product purification and characterization. b) We have not attempted to investigate or identify the nature of the circumstance(s) which give rise to the *N*-methyl

product **24**, but have observed *N*-methylated products on other leads containing nitrogen heterocycles.

64. Electrochemical synthesis of analog **21** was in good agreement chromatographically (HPLC-MS) and spectroscopically (NMR) to compound **21** generated from the BMO control reaction with *m*CPBA (Figure S87 in the Supporting Information).
65. Jeedimalla, N.; Jacquet, C.; Bahneva, D.; Tendoung, J.-J. Y.; Roche, S. P. Synthesis of α-Arylated Cycloalkanones from Congested Trisubstituted Spiro-epoxides: Application of the House–Meinwald Rearrangement for Ring Expansion. *J. Org. Chem.* **2018**, *83*, 12357-12373.
66. a) Tommasino, J.-B.; Brondex, A.; Medebielle, M.; Thomalla, M.; Langlois, B. R.; Billard, T. Trifluoromethylation Reactions with Potassium Trifluoromethanesulfinate Under Electrochemical Oxidation. *Synlett* **2002**, 1697-1699. b) Smertenko, E. A.; Datsenko, S. D.; Ignat'ev, N. V. Electrochemical Oxidation of Sodium Trifluoromethanesulfinate. *Russ. J. Electrochem.* **1998**, *34*, 46-51. c) O'Brien, A. G.; Maruyama, A.; Inokuma, Y.; Fujita, M.; Baran, P. S.; Blackmond, D. G. Radical C-H Functionalization of Heteroarenes Under Electrochemical Control. *Angew. Chem. Int. Ed.* **2014**, *53*, 11868-11871.
67. Villani, F. J. Tricyclic-Substituted Piperidine Antihistamines. U.S. Patent 4,355,036, October 19, 1982.
68. Generation of analog **5** from BM3 variant MCYP-P1.2-D07 gave a superior HPLC-MS chromatographic profile with regards to conversion and impurity profile compared to compound **5** generated from *Streptomyces violascens* ATCC 31560, therefore MCYP-P1.2-D07 was used during the scale-up to prepare analog **8**. Analog **5** from MCYP-P1.2-D07 was in good agreement chromatographically (HPLC-MS) and spectroscopically

(NMR) to compound **5** generated from *Streptomyces violascens* ATCC 3156 (Figure S22 in the Supporting Information).

69. Cheng, Y. C.; Prusoff, W. H. Relationship Between the Inhibition Constant (K_I) and the Concentration of Inhibitor Which Causes 50 Per Cent Inhibition (I_{50}) of an Enzymatic Reaction. *Biochem. Pharmacol.* **1973**, *22*, 3099-3108.
70. Kapinos, B.; Liu, J.; Piotrowski, M.; Keefer, J.; Holder, B.; Janiszewski, J.; Zhang, H.; Troutman, M. Development of a High-Performance, Enterprise-Level, Multimode LC-MS/MS Autosampler for Drug Discovery. *Bioanalysis* **2017**, *9*, 1643-1654.
71. The RRCK cell line is also known as MDCKII-LE. Di, L.; Whitney-Pickett, C.; Umland, J. P.; Zhang, H.; Zhang, X.; Gebhard, D. F.; Lai, Y.; Federico, J. J.; Davidson, R. E.; Smith, R.; Reyner, E. L.; Lee, C.; Feng, B.; Rotter, C.; Varma, M. V.; Kempshall, S.; Fenner, K.; El-Kattan, A. F.; Liston, T. E.; Troutman, M. D. Development of a New Permeability Assay Using Low-Efflux MDCKII Cells. *J. Pharm. Sci.* **2011**, *100*, 4974-4985.
72. CP-628374 (MW 687.04 g/mol): (2E)-3-(4-{[(2S,3S,4S,5R)-5-{(1E)-N-[(3-chloro-2,6-difluorobenzyl)oxy]ethanimidoyl}-3,4-dihydroxytetrahydrofuran-2-yl]oxy}-3-hydroxyphenyl)-2-methyl-N[(3aS,4R,5R,6S,7R,7aR)-4,6,7-trihydroxyhexahydro-1,3-benzodioxol-5-yl]prop-2-enamide. Di, L.; Umland, J. P.; Chang, G.; Huang, Y.; Lin, Z.; Scott, D. O.; Troutman, M. D.; Liston, T. E. Species Independence in Brain Tissue Binding Using Brain Homogenates. *Drug Metab. Dispos.* **2011**, *39*, 1270-1277.

Table of Content graphic.

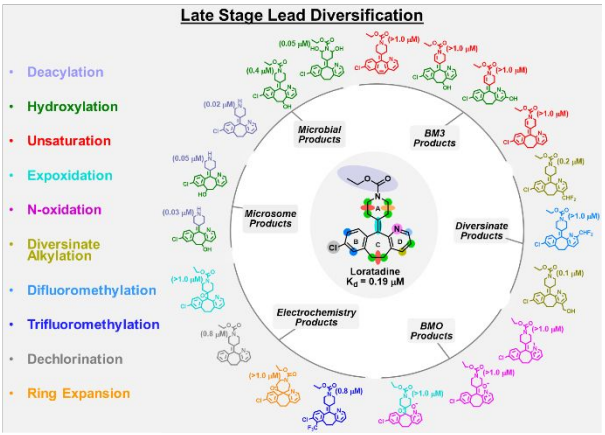

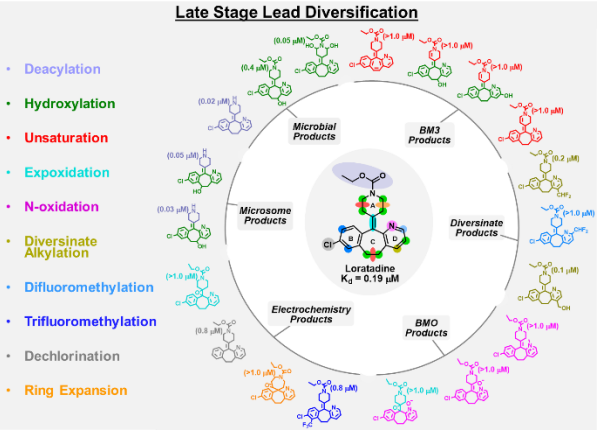
Late Stage Lead Diversification
Deacylation
Hydroxylation
Unsaturation
Expoxidation
N-oxidation
Diversinate Alkylation
Difluoromethylation
Trifluoromethylation
Dechlorination
Ring Expansion
Microbial Products
BM3 Products
Microsome Products
Diversinate Products
Electrochemistry Products
BMO Products
Loratadine
K_d = 0.19 μM